function in an NS3 sequence-dependent manner. J Gen Virol 2006;87:1703–1713.
[21] Lindenbach BD, Evans MJ, Syder AJ, Wolk B, Tellinghuisen TL, Liu CC, et al. Complete replication of hepatitis C virus in cell culture. Science 2005;309:623–626.
[22] Deng L, Adachi T, Kitayama K, Bungyoku Y, Kitazawa S, Ishido S, et al. Hepatitis C virus infection induces apoptosis through a Bax-triggered, mitochondrion-mediated, caspase 3-dependent pathway. J Virol 2008;82:10375–10385.
[23] Kanda H, Tamori Y, Shinoda H, Yoshikawa M, Sakaue M, Udagawa J, et al. Adipocytes from Munc18c-null mice show increased sensitivity to insulin-stimulated GLUT4 externalization. J Clin Invest 2005;115:291–301.
[24] Niwa H, Yamamura K, Miyazaki J. Efficient selection for high-expression transfectants with a novel eukaryotic vector. Gene 1991;108:193–199.
[25] Lehner PJ, Hoer S, Dodd R, Duncan LM. Downregulation of cell surface receptors by the K3 family of viral and cellular ubiquitin E3 ligase. Immunol Rev 2005;207:112–125.
[26] Mehta SH, Brancati FL, Strathdee SA, Pankow JS, Netski D, Coresh J, et al. Hepatitis C virus infection and incident type 2 diabetes. Hepatology 2003;38:50–56.
[27] Wang CS, Wang ST, Yao WJ, Chang TT, Chou P. Hepatitis C virus infection and the development of type 2 diabetes in a community-based longitudinal study. Am J Epidemiol 2007;166:196–203.
[28] Hui JM, Sud A, Farrell GC, Bandara P, Byth K, Kench JG, et al. Insulin resistance is associated with chronic hepatitis C virus infection and fibrosis progression. Gastroenterology 2003;125:1695–1704.
[29] Kawaguchi T, Yoshida T, Harada M, Hisamoto T, Nagao Y, Ide T, et al. Hepatitis C virus down-regulates insulin receptor substrates 1 and 2 through up-regulation of suppressor of cytokine signaling 3. Am J Pathol 2004;165:1499–1508.
[30] Miyamoto H, Moriishi K, Moriya K, Murata S, Tanaka K, Suzuki T, et al. Involvement of the PA28γ-dependent pathway in insulin resistance induced by hepatitis C virus core protein. J Virol 2007;81:1727–1735.
[31] Ader M, Ni TC, Bergman RN. Glucose effectiveness assessed under dynamic and steady state conditions. Comparability of uptake versus production components. J Clin Invest 1997;99:1187–1199.
[32] Banerjee S, Saito K, Ait-Goughoulte M, Meyer K, Ray RB, Ray R. Hepatitis C virus core protein upregulates serine phosphorylation of IRS-1 and impairs downstream Akt/PKB signaling pathway for insulin resistance. J Virol 2008;82:2606–2612.
[33] Im SS, Kim SY, Kim HI, Ahn YH. Transcriptional regulation of glucose sensors in pancreatic beta cells and liver. Curr Diabetes Rev 2006;2:11–18.
[34] Adachi T, Yasuda K, Okamoto Y, Shihara N, Oku A, Ueta K, et al. T-1095, a renal Na^{+}-glucose transporter inhibitor, improves hyperglycemia in streptozotocin-induced diabetic rats. Metabolism 2000;49:990–995.
[35] Im SS, Kang SY, Kim SY, Kim HI, Kim JW, Kim KS, et al. Glucose-stimulated upregulation of GLUT2 gene is mediated by sterol response element-binding protein-1c in the hepatocytes. Diabetes 2005;54:1684–1691.
[36] Kanayama T, Arito M, So K, Hachimura S, Inoue J, Sato R. Interaction between sterol regulatory element-binding proteins and liver receptor homolog-1 reciprocally suppresses their transcriptional activities. J Biol Chem 2007;282:10290–10298.

JOURNAL OF VIROLOGY, Oct. 2008, p. 9639–9646 Vol. 82, No. 19
0022-538X/08/$08.00+0 doi:10.1128/JVI.00351-08

The DNA Damage Sensors Ataxia-Telangiectasia Mutated Kinase and Checkpoint Kinase 2 Are Required for Hepatitis C Virus RNA Replication[▽]

Yasuo Ariumi,[1] Misao Kuroki,[1] Hiromichi Dansako,[1] Ken-Ichi Abe,[1] Masanori Ikeda,[1] Takaji Wakita,[2] and Nobuyuki Kato[1]*

Department of Molecular Biology, Okayama University Graduate School of Medicine, Dentistry, and Pharmaceutical Sciences, 2-5-1, Shikata-cho, Okayama 700-8558, Japan,[1] and Department of Virology II, National Institute of Infectious Diseases, 1-23-1 Toyama, Shinjuku-ku, Tokyo 162-8640, Japan[2]

Received 18 February 2008/Accepted 18 July 2008

Cellular responses to DNA damage are crucial for maintaining genome integrity, virus infection, and preventing the development of cancer. Hepatitis C virus (HCV) infection and the expression of the HCV nonstructural protein NS3 and core protein have been proposed as factors involved in the induction of double-stranded DNA breaks and enhancement of the mutation frequency of cellular genes. Since DNA damage sensors, such as the ataxia-telangiectasia mutated kinase (ATM), ATM- and Rad3-related kinase (ATR), poly(ADP-ribose) polymerase 1 (PARP-1), and checkpoint kinase 2 (Chk2), play central roles in the response to genotoxic stress, we hypothesized that these sensors might affect HCV replication. To test this hypothesis, we examined the level of HCV RNA in HuH-7-derived cells stably expressing short hairpin RNA targeted to ATM, ATR, PARP-1, or Chk2. Consequently, we found that replication of both genome-length HCV RNA (HCV-O, genotype 1b) and the subgenomic replicon RNA were notably suppressed in ATM- or Chk2-knockdown cells. In addition, the RNA replication of HCV-JFH1 (genotype 2a) and the release of core protein into the culture supernatants were suppressed in these knockdown cells after inoculation of the cell culture-generated HCV. Consistent with these observations, ATM kinase inhibitor could suppress the HCV RNA replication. Furthermore, we observed that HCV NS3-NS4A interacted with ATM and that HCV NS5B interacted with both ATM and Chk2. Taken together, these results suggest that the ATM signaling pathway is critical for HCV RNA replication and may represent a novel target for the clinical treatment of patients with chronic hepatitis C.

Hepatitis C virus (HCV) infection frequently causes chronic hepatitis, which progresses to liver cirrhosis and hepatocellular carcinoma. HCV infection has now become a serious health problem, with at least 170 million people currently infected worldwide (28). HCV is an enveloped virus with a positive single-stranded 9.6-kb RNA genome, which encodes a large polyprotein precursor of approximately 3,000 amino acid residues. This polyprotein is cleaved by a combination of the host and viral proteases into at least 10 proteins in the following order: core, envelope 1 (E1), E2, p7, nonstructural 2 (NS2), NS3, NS4A, NS4B, NS5A, and NS5B (12, 13, 27).

Studies have shown that various viruses with distinct replication strategies—including the DNA viruses Epstein-Barr virus, herpes simplex virus 1, adenovirus, and simian virus 40 and the retrovirus human immunodeficiency virus type 1 (HIV-1)—can activate DNA damage response pathways and utilize these damage responses to facilitate their own viral reproduction and promote the survival of infected cells (2, 16, 17). In the case of HCV, it has been proposed that HCV infection causes double-stranded DNA (dsDNA) breaks and enhances the mutation frequency of cellular genes and that these effects are mediated by nitric oxide (18, 19). In addition, the HCV core, E1, and NS3 proteins have been suggested to be potent reactive oxygen species inducers, leading to DNA damage (19). Furthermore, we previously demonstrated that HCV NS5B-expressing PH5CH8 immortalized human hepatocyte cells were susceptible to DNA damage in the form of dsDNA breaks (23). Thus, HCV seems to be associated with the dsDNA damage response pathways.

Since the DNA damage sensors, such as ataxia-telangiectasia mutated kinase (ATM), ATM- and Rad3-related kinase (ATR), poly(ADP-ribose) polymerase 1 (PARP-1), and checkpoint kinase 2 (Chk2; a direct downstream target of ATM), play central roles in response to genotoxic stress (10), we hypothesized that these sensors might affect HCV replication.

To investigate the possible involvement of these cellular factors in HCV replication, we examined the level of HCV RNA in cells rendered defective for DNA damage sensors by RNA interference or by pharmacological inhibition.

MATERIALS AND METHODS

Cell culture. 293FT cells were cultured in Dulbecco's modified Eagle's medium (DMEM; Invitrogen, Carlsbad, CA) supplemented with 10% fetal bovine serum (FBS). The HuH-7-derived O cells harboring a replicative genome-length HCV RNA and the HuH-7-derived sO cells harboring the subgenomic replicon RNA of HCV-O were cultured in DMEM with 10% FBS and G418 (300 μg/ml geneticin; Invitrogen) as described previously (11, 14). Oc and sOc cells, which were created by eliminating HCV RNA from O cells and sO cells by interferon (IFN) treatment (11, 14), respectively, were also cultured in DMEM with 10% FBS.

RNA interference. Oligonucleotides with the following sense and antisense sequences were used for the cloning of short hairpin RNA (shRNA)-encoding se-

* Corresponding author. Mailing address: Department of Molecular Biology, Okayama University Graduate School of Medicine, Dentistry, and Pharmaceutical Sciences, 2-5-1, Shikata-cho, Okayama 700-8558, Japan. Phone: 81 86 235 7385. Fax: 81 86 235 7392. E-mail: nkato@md.okayama-u.ac.jp.

▽ Published ahead of print on 30 July 2008.

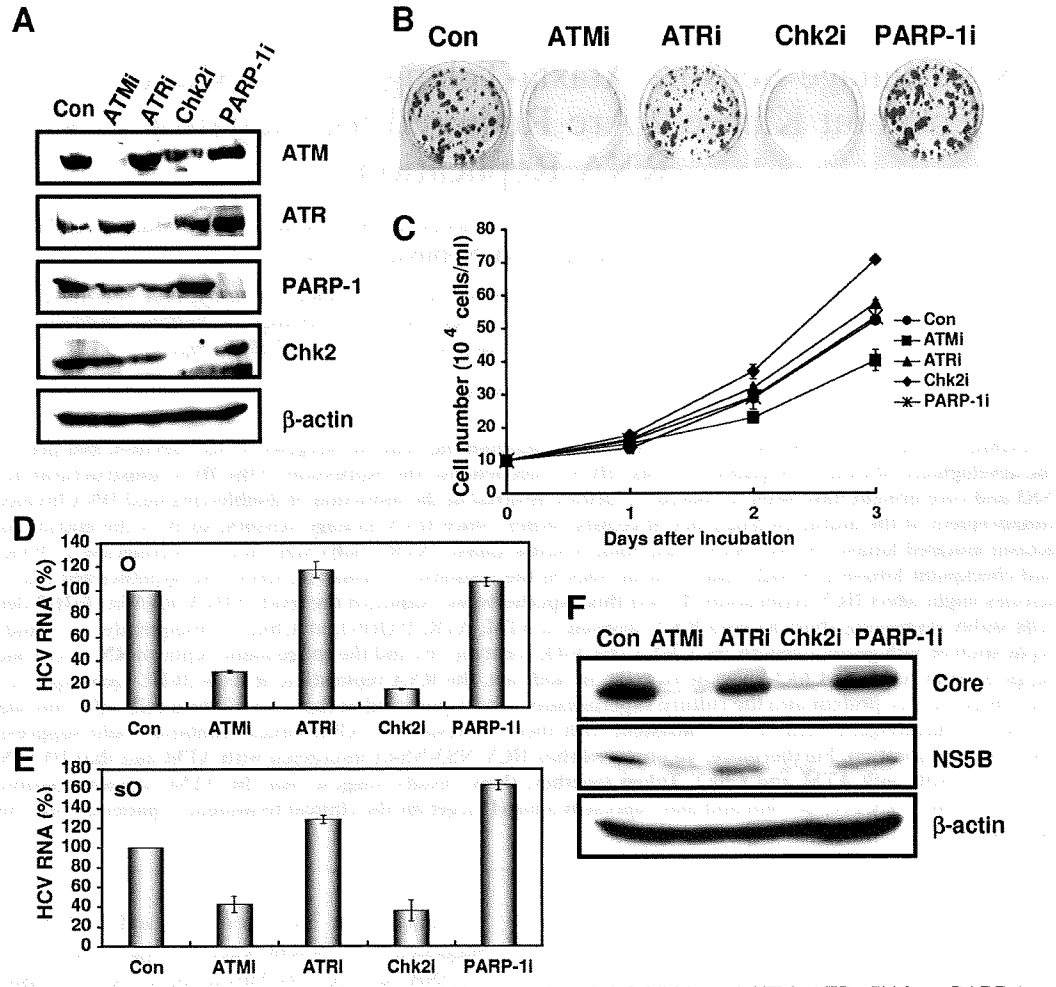

FIG. 1. The ATM signaling pathway is required for HCV RNA replication. (A) Inhibition of ATM, ATR, Chk2, or PARP-1 expression by shRNA-producing lentiviral vectors. The results of the Western blot analysis of cellular lysates with anti-ATM, anti-ATR, anti-Chk2, anti-PARP-1, or anti-β-actin antibody in Oc cells expressing shRNA targeted to ATM (ATMi), ATR (ATRi), Chk2 (Chk2i), or PARP-1 (PARP-1i) as well as in Oc cells transduced with a control lentiviral vector (Con) are shown. (B) ECF in ATM-, ATR-, Chk2-, or PARP-1-knockdown cells. In vitro transcribed ON/C-5B K1609E RNA (2 μg) was transfected into the ATM-, ATR-, Chk2, or PARP-1-knockdown Oc cells or the Oc cells transduced with a control lentiviral vector (Con). G418-resistant colonies were stained with Coomassie brilliant blue at 3 weeks after electroporation of RNA. Experiments were done in duplicate, and a representative result is shown. (C) The cell growth curve of ATM (ATMi), ATR (ATRi), Chk2 (Chk2i), or PARP-1 (PARP-1i)-knockdown Oc cells or the Oc cells transduced with a control lentiviral vector (Con). Results from three independent experiments are shown. (D) The level of genome-length HCV-O RNA was monitored by real-time LightCycler PCR (Roche). Experiments were done in triplicate, and columns represent the mean percentage of HCV RNA. (E) The level of subgenomic replicon (sO cells) RNA was monitored by real-time LightCycler PCR. Results from three independent experiments are shown as described in panel D. (F) The HCV core or NS5B protein expression level in ATM-, ATR-, Chk2-, or PARP-1-knockdown cells. The results of Western blot analysis of cellular lysates with anti-HCV core protein, anti-HCV NS5B, or anti-β-actin antibody in O cells expressing shRNA targeted to ATM (ATMi), ATR (ATRi), Chk2 (Chk2i), or PARP-1 (PARP-1i) as well as in O cells transduced with a control lentiviral vector (Con) are shown.

quences targeted to Chk2 in lentiviral vector: 5′-GATCCCCGGGGGAGAGCTGTT TGACATTCAAGAGATGTCAAACAGCTCTCCCCCTTTTTGGAAA-3′ (sense) and 5′-AGCTTTTCCAAAAAGGGGGAGAGCTGTTTGACATCTCTTGAATGT CAAACAGCTCTCCCCCGGG-3′ (antisense). The oligonucleotides above were annealed and subcloned into the BglII-HindIII site, downstream from an RNA polymerase III promoter of pSUPER (5), generating pSUPER-Chk2i. To construct pLV-Chk2i, the BamHI-SalI fragments of the pSUPER-Chk2i were subcloned into the BamHI-SalI site of pRDI292, an HIV-1-derived self-inactivating lentiviral vector containing a puromycin resistance marker allowing for the selection of transduced cells (4). pLV-ATMi, pLV-ATRi, and pLV-PARP-1i were constructed as described previously (1).

Lentiviral vector production. The vesicular stomatitis virus G protein (VSV-G)-pseudotyped HIV-1-based vector system has been described previously (24). The lentiviral vector particles were produced by transient transfection of the second-generation packaging construct pCMV-ΔR8.91 (30) and the VSV-G envelope plasmid pMDG2 as well as the lentiviral vector into 293FT cells with FuGene6 (Roche Diagnostics, Mannheim, Germany).

Quantitative reverse transcription-PCR analysis. Quantitative reverse transcription-PCR analysis for HCV RNA was performed by real-time LightCycler PCR as described previously (11).

Western blot analysis. Cells were lysed in buffer containing 50 mM Tris-HCl (pH 8.0), 150 mM NaCl, 4 mM EDTA, 1% Nonidet P-40, 0.1% sodium dodecyl sulfate (SDS), 1 mM dithiothreitol, and 1 mM phenylmethylsulfonyl fluoride. Supernatants from these lysates were subjected to SDS-polyacrylamide gel electrophoresis, followed by immunoblotting analysis using anti-ATM (2C1; GTX70103 [GeneTex, San Antonio, TX]), anti-ATR (GTX70133; GeneTex), anti-Chk2 (NT; ProSci, Poway, CA), anti-Chk2 (DCS-273; Medical and Biological Laboratories, Nagoya, Japan), anti-phospho-Chk2 (Thr68) (Cell Signaling,

Danvers, MA), anti-PARP-1 (C-2-10; Calbiochem, Merck Biosciences, Darmstadt, Germany), anti-hemagglutinin (HA) (HA-7; Sigma, St. Louis, MO), anti-core protein (CP-9 and CP-11; Institute of Immunology, Tokyo, Japan), anti-NS3 and anti-NS5B (no. 14; a generous gift from M. Kohara, the Tokyo Metropolitan Institute of Medical Science, Japan), anti-NS5A (no. 8926; a generous gift from A. Takamizawa, The Research Foundation for Microbial Diseases of Osaka University, Japan), and anti-β-actin (Sigma) Antibodies.

Immunofluorescence and confocal microscopic analysis. Cells were fixed in 3.5% formaldehyde in phosphate-buffered saline (PBS) and permeabilized in 0.1% NP-40 in PBS at room temperature. Cells were incubated with anti-ATM antibody (5C2; GTX70107 [GeneTex] or PM026 [MBL]), anti-HA antibody (3F10), anti-NS5B antibody and/or anti-NS3 antibody at a 1:300 dilution in PBS containing 3% bovine serum albumin at 37°C for 30 min. Cells were then stained with fluorescein isothiocyanate (FITC)-conjugated anti-rabbit antibody (Jackson ImmunoResearch, West Grove, PA) or anti-Cy3-conjugated anti-mouse antibody (Jackson ImmunoResearch) at a 1:300 dilution in PBS containing bovine serum albumin at 37°C for 30 min. Following extensive washing in PBS, cells were mounted on slides using a mounting medium of 90% glycerin–10% PBS with 0.01% *p*-phenylenediamine added to reduce fading. Samples were viewed under a confocal laser-scanning microscope (LSM510; Zeiss, Jena, Germany).

Immunoprecipitation. Cells were lysed in buffer containing 10 mM Tris-HCl (pH 8.0), 150 mM NaCl, 4 mM EDTA, 0.5% NP-40, 10 mM NaF, 1 mM dithiothreitol, and 1 mM phenylmethylsulfonyl fluoride. Lysates were precleared with 30 μl of protein G-Sepharose (GE Healthcare Biosciences, Uppsala, Sweden). Precleared supernatants were incubated with 5 μg of anti-HA antibody (3F10; Roche), 10 μl of anti-NS5B antibody, 5 μg of anti-Chk2 antibody (DCS-273; MBL), 5 μg of anti-FLAG antibody (M2; Sigma), or 5 μg of anti-ATM antibody (2C1) (GTX70103; GeneTex) at 4°C for 1 h. Following absorption of the precipitates on 30 μl of protein G-Sepharose resin for 1 h, the resin was washed four times with 700 μl of lysis buffer. Proteins were eluted by boiling the resin for 5 min in 2× Laemmli sample buffer. The proteins were then subjected to SDS-polyacrylamide gel electrophoresis, followed by immunoblotting analysis using anti-ATM, anti-Chk2, anti-HCV core protein (CP-9 and CP-11 mixture), anti-NS5A, anti-NS5B, anti-HA (HA-7; Sigma), or anti-NS3 antibody.

RESULTS

ATM and Chk2 are required for HCV RNA replication. To determine the potential role of DNA damage sensors in HCV replication, we first used lentiviral vector-mediated RNA interference to stably knockdown ATM, ATR, PARP-1 (1), or Chk2 in the following human hepatoma HuH-7-derived cell lines: O cells harboring a replicative genome-length HCV RNA (HCV-O, genotype 1b) (11), Oc cells derived from O cells (created by eliminating genome-length HCV RNA from O cells by IFN treatment) (11), sO cells harboring the subgenomic replicon of HCV-O (14), or RSc cells that cell culture-generated HCV (HCVcc) (JFH1, genotype 2a) (29) could infect and effectively replicate (3). To express shRNAs targeted to ATM, ATR, PARP-1 (1), or Chk2, we used a VSV-G-pseudotyped HIV-1-based vector system (24). We used puromycin-resistant pooled cells 10 days after the lentiviral transduction in all experiments. Western blot analysis of the lysates demonstrated very effective knockdown of ATM, ATR, Chk2, and PARP-1 in Oc cells (Fig. 1A). The effective knockdown of ATM, ATR, Chk2, or PARP-1 in O cells or sO cells was also confirmed by Western blot analysis (data not shown). In this context, the efficiency of colony formation (ECF) in ATM- or Chk2-, but not ATR- or PARP-1-, knockdown Oc cells transfected with the genome-length HCV-O RNA with an adapted mutation at amino acid position 1609 in the NS3 helicase region (ON/C-5B K1609E RNA) (11) was notably reduced compared with the control cells (Fig. 1B) even though Chk2-knockdown cells had a slightly faster growth rate than the control cells (Fig. 1C), suggesting that both ATM and Chk2 are crucial for HCV RNA replication. To further confirm this

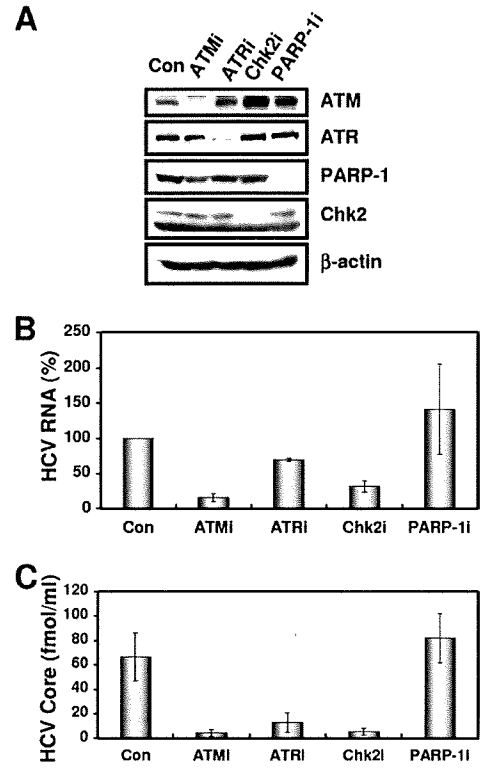

FIG. 2. ATM affects HCV infection. (A) Inhibition of ATM, ATR, Chk2, or PARP-1 expression by shRNA-producing lentiviral vectors. The results of Western blot analysis of cellular lysates with anti-ATM, anti-ATR, anti-PARP-1, anti-Chk2, or anti-β-actin antibody in RSc cured cells expressing shRNA targeted to ATM (ATMi), ATR (ATRi), Chk2 (Chk2i), or PARP-1 (PARP-1i) as well as in RSc cells transduced with a control lentiviral vector (Con) are shown. (B) The level of genome-length HCV (JFH1) RNA was monitored by real-time LightCycler PCR after inoculation of the HCVcc. Results from three independent experiments are shown as described in the legend of Fig. 1D. (C) The levels of the core protein in the culture supernatants were determined by enzyme-linked immunosorbent assay (Mitsubishi Kagaku Bio-Clinical Laboratories). Experiments were done in triplicate, and columns represent the mean core protein levels.

observation, we quantitatively examined the level of HCV RNA in the O cell- or sO cell-derived knockdown cells. Consequently, we found that replication of both genome-length HCV RNA (HCV-O) and its subgenomic replicon RNA (sO) were notably suppressed in ATM- or Chk2-knockdown cells but not in ATR- or PARP-1-knockdown cells (Fig. 1D and E). Consistent with this finding, the expression levels of core and NS5B proteins were also significantly decreased in the cell lysates of ATM- or Chk2-knockdown O cells (Fig. 1F). We next examined the replication level of HCV-JFH1 in ATM-, ATR-, Chk2-, or PARP-1-knockdown RSc cells (Fig. 2A). The results revealed that RNA replication of HCV-JFH1 and release of core protein into the culture supernatants were suppressed in only ATM- or Chk2-knockdown RSc cells after inoculation with HCVcc (Fig. 2B and C). Interestingly, the release of core protein into the culture supernatant was also significantly suppressed in ATR-knockdown RSc cells, while HCV RNA replication was slightly suppressed in these cells

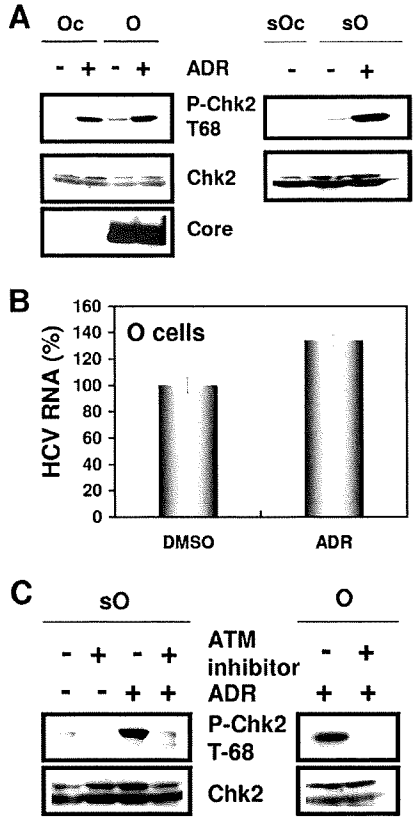

FIG. 3. ATM-dependent DNA damage response in HCV RNA-replicating cells. (A) Stimulation of Chk2 phosphorylation in the HCV RNA-replicating cells. The Oc, O, or sO cells were treated with 100 nM adriamycin (Sigma) for 2 h. The results of Western blot analysis of cellular lysates with anti-phospho-Chk2 (Thr68) (P-Chk2 T68), anti-Chk2, or anti-core protein antibody are shown. (B) Effect of adriamycin on HCV RNA replication. The O cells were treated with 100 nM adriamycin for 24 h. The level of genome-length HCV-O RNA was monitored by real-time LightCycler PCR. Results from three independent experiments are shown as described in the legend of Fig. 1D. DMSO, dimethyl sulfoxide. (C) Effect of ATM kinase inhibitor on Chk2 phosphorylation. The sO or O cells were pretreated with 10 μM ATM kinase inhibitor (KU-55933) (Calbiochem) for 2 h, followed by treatment with 100 nM adriamycin for 2 h. The results of Western blot analysis of cellular lysates with anti-phospho-Chk2 (Thr68) or anti-Chk2 antibody are shown.

(Fig. 2B and C), suggesting that ATR participates in the production of HCV virion.

In contrast, highly efficient knockdown of PARP-1 had no observable effects on the ECF (Fig. 1B), HCV RNA replication (Fig. 1D and E and 2B), or core protein expression in the cell lysate or in the supernatant (Fig. 1F and 2C), suggesting that our finding was not due to a nonspecific event. Thus, we have demonstrated for the first time that DNA damage sensors, ATM and Chk2, are required for HCV RNA replication.

ATM kinase activity in HCV RNA-replicating cells. Although it has been proposed that HCV causes dsDNA breaks (18, 19), little is known about whether HCV activates or inhibits the ATM-dependent damage response pathway. In this regard, it is worth noting that we observed weak but significant Chk2 phosphorylation at threonine 68, the specific marker for

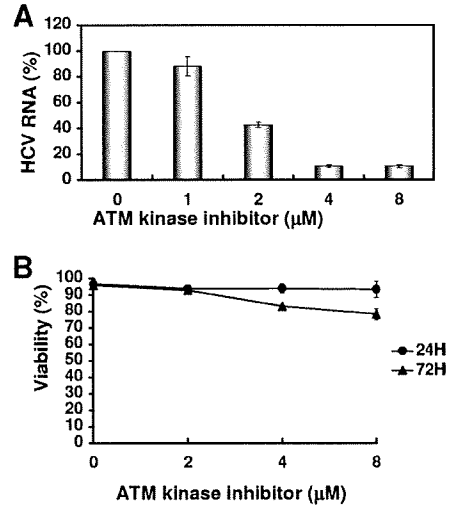

FIG. 4. Suppression of HCV RNA replication by ATM kinase inhibitor. (A) The level of genome-length HCV-O RNA was monitored by real-time LightCycler PCR after treatment with the indicated concentration of ATM kinase inhibitor for 72 h. Results from three independent experiments are shown as described in the legend of Fig. 1D. (B) Cell viabilities after treatment with the indicated concentration of ATM kinase inhibitor for 24 h or 72 h are shown.

ATM activation (20, 21), in the HCV RNA-replicating cells (O and sO cells) but not in the HCV-negative Oc and sOc cells (created by eliminating replicon RNA from sO cells by IFN treatment) (Fig. 3A), suggesting that the persistent HCV RNA replication stimulated the ATM-dependent DNA damage response. Furthermore, a 2-h treatment with 100 nM adriamycin, a dsDNA break inducer, markedly induced Chk2 phosphorylation in Oc, O, and sO cells (Fig. 3A). Importantly, Chk2 phosphorylation was not inhibited even in the HCV RNA-replicating cells (O and sO cells) (Fig. 3A), suggesting that the persistent HCV RNA replication and the HCV proteins are not able to suppress the ATM-dependent DNA damage response. To examine whether such a DNA damage response activates HCV RNA replication, we quantified the level of HCV RNA in the O cells treated with 100 nM adriamycin for 24 h. The results show that HCV RNA replication was increased (approximately 1.3-fold) after treatment with adriamycin (Fig. 3B), suggesting that the DNA damage response activates HCV RNA replication.

Suppression of HCV RNA replication by a small-molecule inhibitor of the ATM kinase. We next examined the effect of a specific small-molecule inhibitor of the ATM kinase (2-morpholin-4-yl-6-thianthren-1-yl-pyran-4-one [KU-55933]) (16) on HCV RNA replication. As expected, the ATM kinase inhibitor effectively inhibited Chk2 phosphorylation after adriamycin treatment in both sO and O cells (Fig. 3C). In this context, the ATM kinase inhibitor could efficiently suppress genome-length HCV RNA replication with an in vitro 50% effective concentration (EC_{50}) of approximately 2 μM at 72 h after treatment with adriamycin (Fig. 4A). Although this ATM kinase inhibitor did not affect cell viability at 24 h after the treatment, there was a slight decrease in the cell viability at 72 h after treatment (Fig. 4B). Thus, this or other ATM kinase inhibitors may be

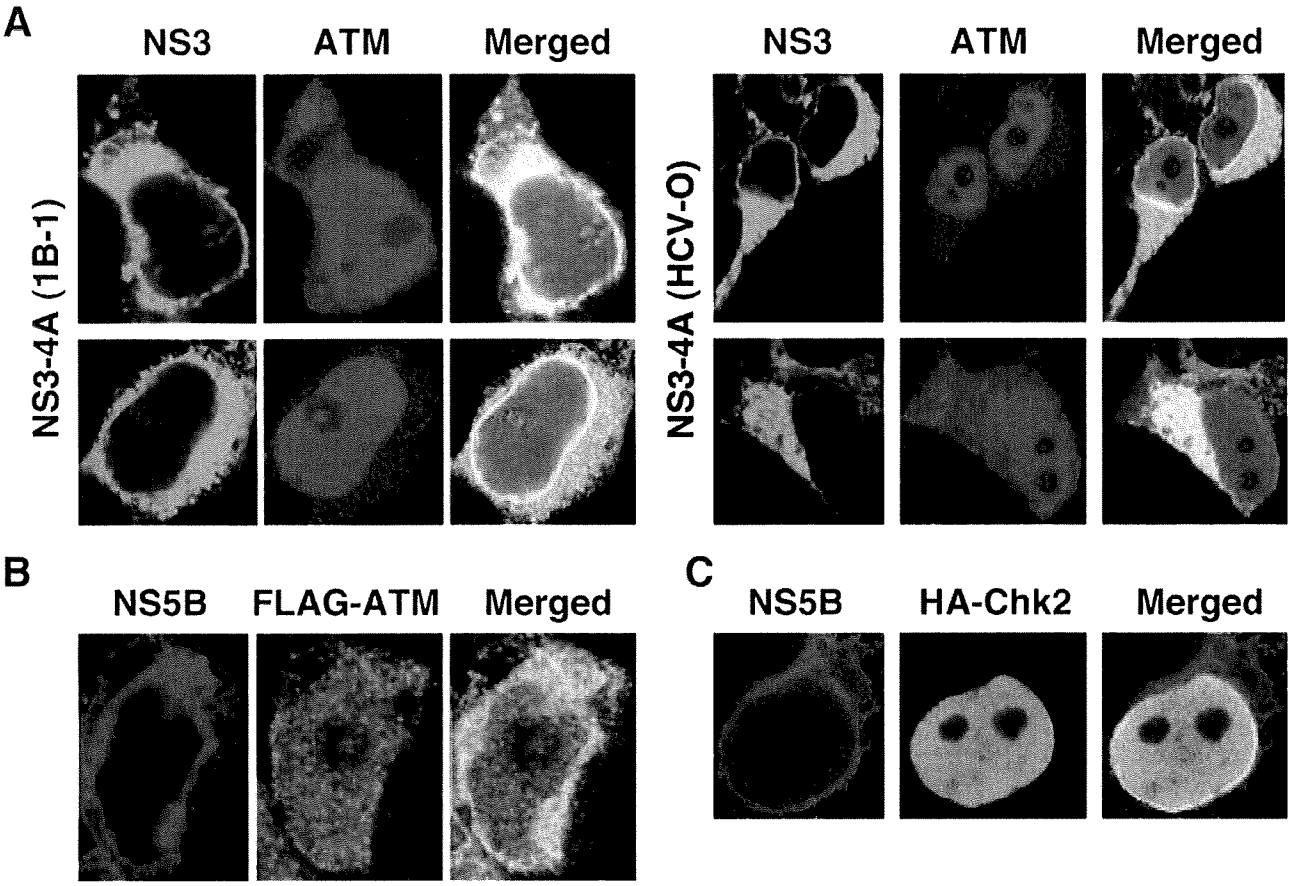

FIG. 5. Subcellular localization of ATM and Chk2 in HCV NS3-4A- or NS5B-expressing cells. (A) ATM partially colocalized with HCV NS3-4A. 293FT cells cotransfected with 300 ng of pCX4bsr/NS3-4A (1B-1) (8) or pCX4bsr/NS3-4A (O) (8) and 300 ng of pcDNA3-FLAG-ATMwt (6) were examined by confocal laser scanning microscopy. Cells were stained with anti-NS3 and anti-ATM (5C2) antibodies and then visualized with FITC (NS3) or Cy3 (ATM). (B) ATM partially colocalized with HCV NS5B. 293FT cells cotransfected with 300 ng of pCX4bsr/NS5B (1B-1) (23) and 300 ng of pcDNA3-FLAG-ATMwt (6). Cells were stained with anti-NS5B (no. 14) and anti-ATM (PM026) antibodies and then visualized with FITC (ATM) or Cy3 (NS5B). (C) Chk2 partially colocalized with HCV NS5B. 293FT cells cotransfected with 300 ng of pCX4bsr/NS5B (1B-1) (23) and 300 ng of pcDNA3-HA-Chk2wt (20, 21). Cells were stained with anti-NS5B and anti-HA (3F10) antibodies and then visualized with FITC (HA-Chk2) or Cy3 (NS5B). Images were visualized using confocal laser scanning microscopy (LSM510; Carl Zeiss). The right panels exhibit two-color overlay images (Merged). Colocalization is shown in yellow.

useful for the clinical treatment of patients with chronic hepatitis C.

Interaction of HCV NS3-4A with ATM. Since HCV NS3 has been proposed to be a viral factor involved in the induction of dsDNA breaks (18, 19), we first examined the subcellular localization of NS3-NS4A ([NS3-4A] 1B-1 or HCV-O strain) and ATM by confocal laser scanning microscopy. In most of the observed cells, ATM partially colocalized with NS3-4A in the perinuclear region and in dispersed points throughout the cytoplasm (Fig. 5A). In particular, we observed prominent colocalization of ATM with NS3-4A in some cells (Fig. 5A). Next, using anti-FLAG and anti-ATM antibodies, we immunoprecipitated lysates from 293FT cells in which FLAG-tagged ATM and either NS3-4A (HCV-O) or NS3 (HCV-O) were overexpressed and then performed immunoblotting analysis using either anti-ATM or anti-NS3 antibody to determine whether ATM binds to NS3-4A or NS3. The results revealed that ATM preferentially bound to NS3-4A over NS3 alone (Fig. 6A). Similarly, we found that ATM bound to NS3-4A using the O cell lysates (Fig. 6B), while HA-tagged Chk2 did not bind to NS3-4A in immunoprecipitation analysis using lysates from 293FT cells in which NS3-4A and HA-tagged Chk2 were overexpressed (Fig. 6C). Although NS3-4A has protease activity, ATM was not cleaved by the NS3-4A protease (Fig. 6D). Taking these results together, we conclude that ATM is able to interact with NS3-4A.

Interaction of HCV NS5B with ATM and Chk2. We next examined the subcellular localization of ATM and/or Chk2 in HCV NS5B-expressing cells by confocal laser scanning microscopy since we previously demonstrated that HCV NS5B-expressing PH5CH8 immortalized human hepatocyte cells were susceptible to DNA damage in the form of dsDNA breaks (23). ATM partially colocalized with NS5B in dispersed points throughout the cytoplasm (Fig. 5B), similar to the subcellular localization of HCV NS3-4A and ATM. Furthermore, Chk2 also partially colocalized with NS5B in the perinuclear region and in dispersed points in the nucleus (Fig. 5C). To determine whether endogenous ATM binds to NS5B, lysates from Oc or

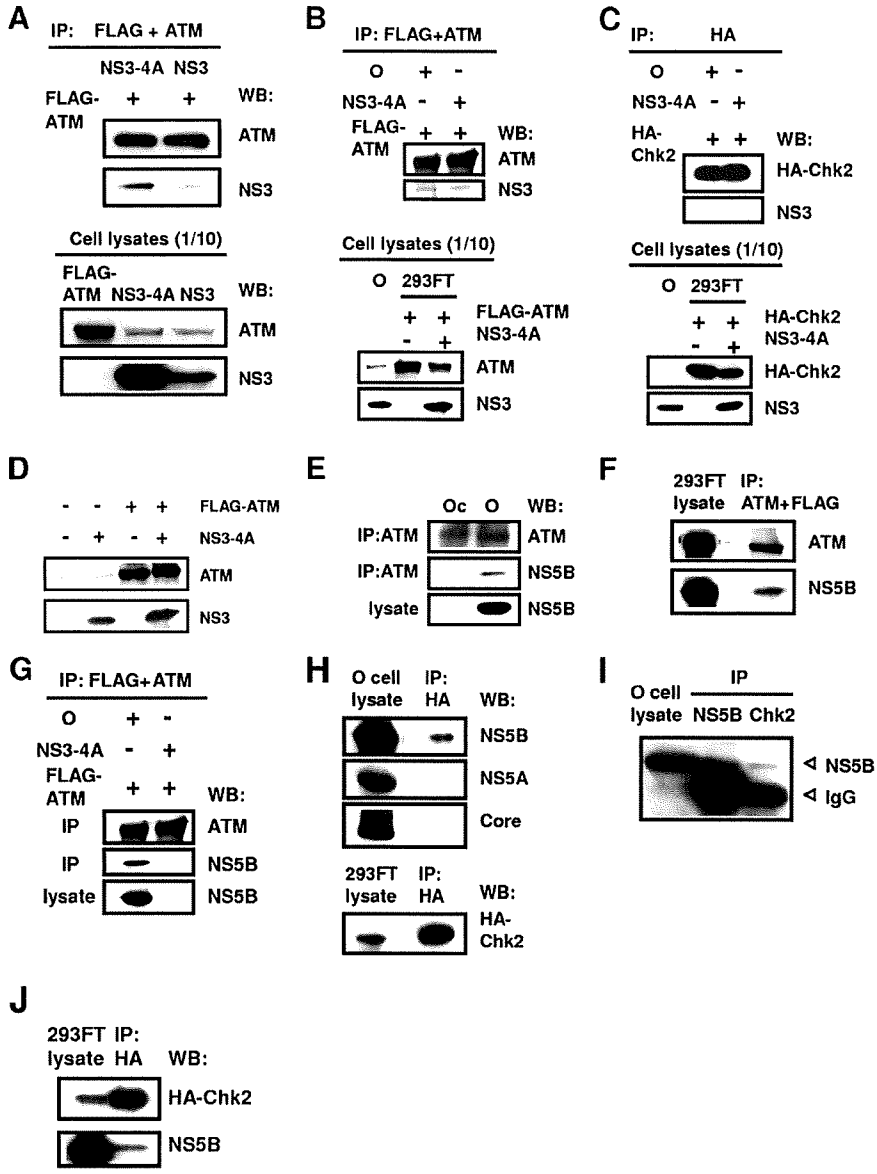

FIG. 6. Interaction of HCV NS3-4A and NS5B with the ATM signaling pathway. (A and B) ATM bound to HCV NS3-4A. (A) 293FT cells were transfected with 4 μg of pCX4bsr/NS3-4A (O), 4 μg of pCX4bsr/NS3 (O), or 4 μg of pcDNA3-FLAG-ATMwt. The cell lysates of expressed FLAG-ATM were mixed with lysates expressing either NS3-4A or NS3. The cell lysates were immunoprecipitated with both anti-FLAG (M2) and anti-ATM (2C1) antibodies, followed by immunoblotting analysis using either anti-ATM (2C1) or anti-HCV NS3 antibody. The results of Western blot analysis of 1/10 of the cellular lysates with anti-ATM or anti-NS3 antibody are also shown. (B) 293FT cells were cotransfected with 4 μg of pcDNA3-FLAG-ATMwt and/or 4 μg of pCX4bsr/NS3-4A (O). The cell lysates of expressed FLAG-ATM alone were mixed with the O cell lysates. Immunoprecipitation and Western blot analysis were performed as described in panel A. (C) Chk2 did not bind to NS3-4A. 293FT cells were cotransfected with 4 μg of pcDNA3-HA-Chk2wt and/or 4 μg of pCX4bsr/NS3-4A (O). The cell lysates of expressed HA-Chk2 alone were mixed with the O cell lysates. The cell lysates were immunoprecipitated with anti-HA antibody (3F10), followed by Western blot analysis using either anti-HA (HA-7) or anti-HCV NS3 antibody. The results of Western blot analysis of 1/10 of the cellular lysates with anti-HA or anti-NS3 antibody are also shown. (D) ATM was not cleaved by HCV NS3-4A protease. 293FT cells were cotransfected with 4 μg of pCX4bsr/NS3-4A (O) and/or 4 μg of pcDNA3-FLAG-ATMwt. The results of Western blot analysis of cellular lysates with anti-ATM or anti-NS3 antibody are shown. (E to G) ATM bound to HCV NS5B. (E) The lysates of O or Oc cells were immunoprecipitated with anti-ATM antibody (2C1), followed by immunoblotting analysis using either anti-ATM or anti-HCV NS5B antibody (no. 14). The results of Western blot analysis of 1/10 of the cellular lysates with anti-NS5B antibody are also shown. (F) 293FT cells were cotransfected with 4 μg of pCX4bsr/NS5B (1B-1) and 4 μg of pcDNA3-FLAG-ATMwt. The cell lysates were immunoprecipitated with both anti-FLAG and anti-ATM antibodies, followed by immunoblotting analysis using either anti-ATM or anti-HCV NS5B antibody. (G) Western Blot analysis was performed with anti-NS5B antibody, reusing the same blotted membrane that was used for panel B. (H to J) Chk2 bound to HCV NS5B. (H) 293FT cells were cotransfected with 4 μg of pcDNA3-HA-Chk2wt. The cell lysates of expressed HA-Chk2 were mixed with the O cell lysates and were immunoprecipitated with anti-HA antibody (3F10), followed by immunoblotting analysis using anti-HCV NS5B, anti-HCV NS5A (no. 8926), anti-HCV core protein (CP-9 and CP-11 mixture), or anti-HA (HA-7) antibody. The results of Western blot analysis of 1/10 of the cellular lysates with the same antibodies are also shown. (I) The lysates of O cells were immunoprecipitated with anti-NS5B or anti-Chk2 antibody (DCS-273), followed by immunoblotting analysis using anti-HCV NS5B antibody. The result of Western blot analysis of 1/10 of the cellular lysates with anti-NS5B antibody is also shown. (J) 293FT cells were cotransfected with 4 μg of pCX4bsr/NS5B (1B-1) and 4 μg of pcDNA3-HA-Chk2wt. The cell lysates were immunoprecipitated with anti-HA antibody (3F10), followed by immunoblotting analysis using either anti-HA (HA-7) or anti-HCV NS5B antibody. IP, immunoprecipitation; WB, Western blotting; IgG, immunoglobulin G.

O cells were immunoprecipitated with anti-ATM antibody, and then immunoblotting analysis using either anti-ATM or anti-NS5B antibody was performed. The results revealed that endogenous ATM bound to endogenous NS5B (Fig. 6E). Furthermore, we confirmed that ATM bound to NS5B in immunoprecipitation analysis using lysates from 293FT cells, in which NS5B (1B-1 strain) and FLAG-tagged ATM were overexpressed (Fig. 6F). Similarly, we confirmed that FLAG-tagged ATM bound to NS5B derived from O cell lysates in immunoprecipitation analysis using lysates from 293FT cells in which FLAG-tagged ATM was overexpressed (Fig. 6G). Finally, to determine which HCV protein binds to Chk2, the 293FT cell lysates of overexpressed HA-Chk2 were mixed with the O cell lysates and were immunoprecipitated with anti-HA antibody, followed by Western blot analysis using anti-HCV NS5B, anti-HCV NS5A, anti-HCV core protein, or anti-HA antibody. Consistent with the immunofluorescence result that Chk2 partially colocalized with NS5B (Fig. 5C), we observed that HA-tagged Chk2 bound to NS5B (Fig. 6H). Importantly, we found that endogenous Chk2 bound to endogenous NS5B derived from O cells (Fig. 6I). In addition, HA-tagged Chk2 bound to NS5B in immunoprecipitation analysis using lysates from 293FT cells in which NS5B (1B-1 strain) and HA-tagged Chk2 were overexpressed (Fig. 6J). Thus, Chk2 also interacted with NS5B as well as ATM. Taking these results together, we conclude that HCV targets ATM and Chk2 DNA damage sensors and that the ATM signaling pathway is required for HCV RNA replication.

DISCUSSION

ATM has been implicated as a target of most DNA viruses, harboring their genomes in the form of dsDNA which can activate or inhibit the ATM signaling pathway (17). In this study, we have demonstrated for the first time that the ATM signaling pathway is required for HCV RNA replication even though HCV does not have a dsDNA genome, unlike DNA viruses. In this regard, Machida et al. previously proposed that HCV infection and the expression of HCV NS3 and core protein induced dsDNA breaks (18, 19). Furthermore, NS3 has DNA helicase activity by which it unwinds dsDNA, suggesting that NS3 affects host dsDNA (22, 25). Thus, HCV infection might trigger the activation of ATM without a dsDNA genome. In fact, we observed weak but significant phosphorylation of Chk2 at threonine 68, the specific marker for ATM activation, in the HCV RNA-replicating cells (O and sO cells) but not in the HCV-negative Oc and sOc cells (Fig. 3A), suggesting that the ATM-dependent DNA damage response is constantly stimulated in persistent HCV RNA-replicating cells. Furthermore, we demonstrated that ATM preferentially bound to NS3-4A over NS3 alone (Fig. 5B) and that ATM partially colocalized with NS3-4A in the perinuclear region, where HCV is known to form a replication complex and replicate itself, and in dispersed points throughout the cytoplasm (Fig. 5A), indicating the interaction of ATM with NS3-4A. Interestingly, Lai et al. very recently reported that NS3-4A impaired DNA repair and enhanced sensitivity to ionizing radiation through interaction with ATM (15). However, we observed an equivalent level of Chk2 phosphorylation at threonine 68, a direct downstream target of ATM (20, 21), in both HCV RNA-replicating cells (O cells) and HCV-negative cells (Oc cells) after treatment with adriamycin (Fig. 3A), suggesting that Chk2 phosphorylation by ATM is not impaired by HCV RNA replication. In this regard, Gaspar and Shenk also showed that human cytomegalovirus could inhibit a DNA damage response by mislocalizing ATM and phosphorylated Chk2 at threonine 68 to a cytoplasmic virus assembly zone, indicating that human cytomegalovirus blocked at the level of Chk2 (9). On the other hand, dsDNA triggers IFN immune defenses through retinoic acid-induced gene I, the mitochondrial antiviral signaling protein, or the DNA-dependent activator of IFN-regulatory factor (7, 26); and NS3-4A protease, which is known to cleave the mitochondrial antiviral signaling protein, can block it (26), suggesting that interaction of NS3-4A with ATM is partially involved in such a common antiviral signaling pathway. On the other hand, we previously demonstrated that HCV NS5B-expressing PH5CH8 immortalized human hepatocyte cells were susceptible to DNA damage in the form of dsDNA breaks (23). In this regard, we have found that HCV NS5B could bind to both ATM and Chk2 (Fig. 5B and C and 6E to J). Together, these results indicate that HCV might hijack ATM and Chk2 and utilize ATM and Chk2 for HCV RNA replication, thereby resulting in impairment of DNA repair, enhancement of mutation frequency, and development of hepatocellular carcinoma.

Finally, consistent with our finding that ATM was required for HCV RNA replication, an ATM kinase inhibitor efficiently suppressed genome-length HCV RNA replication at an EC_{50} of approximately 2 μM at 72 h after the treatment (Fig. 4A). Similarly, Lau et al. reported that the same ATM kinase inhibitor could suppress HIV-1 replication at an EC_{50} of approximately 2.3 μM (16). Importantly, the EC_{50} for HIV-1 replication is similar to that for HCV replication. Thus, this or other ATM kinase inhibitors may represent a novel approach for the clinical treatment of patients with chronic hepatitis C as well as AIDS patients.

ACKNOWLEDGMENTS

We thank D. Trono, R. Agami, R. Iggo, M. Kastan, S. J. Elledge, M. Kohara, A. Takamizawa, and M. Hijikata for the VSV-G-pseudotyped HIV-1-based vector system (pCMVR8.91 and pMDG2) and for pSUPER, pRDI292, pcDNA3-FLAG-ATM, and pcDNA3-HA-Chk2, and for anti-NS3 antibody, anti-NS5B antibody, anti-NS5A antibody, and 293FT cells. We also thank A. Morishita and T. Nakamura for their technical assistance.

This work was supported by a Grant-in-Aid for Young Scientists (B) from the Ministry of Education, Culture, Sports, Science and Technology (MEXT); by a Grant-in-Aid for Research on Hepatitis from the Ministry of Health, Labor, and Welfare of Japan; by the Ichiro Kanehara Foundation; and by a Research Fellowship from the Japan Society for the Promotion of Science.

REFERENCES

1. **Ariumi, Y., P. Turelli, M. Masutani, and D. Trono.** 2005. DNA damage sensors ATM, ATR, DNA-PKcs, and PARP-1 are dispensable for human immunodeficiency virus type 1 integration. J. Virol. **79**:2973–2978.
2. **Ariumi, Y., and D. Trono.** 2006. Ataxia-telangiectasia-mutated (ATM) protein can enhance human immunodeficiency virus type 1 replication by stimulating Rev. function. J. Virol. **80**:2445–2452.
3. **Ariumi, Y., M. Kuroki, K. Abe, H. Dansako, M. Ikeda, T. Wakita, and N. Kato.** 2007. DDX3 DEAD-box RNA helicase is required for hepatitis C virus RNA replication. J. Virol. **81**:13922–13926.
4. **Bridge, A. J., S. Pebernard, A. Ducraux, A.-L. Nicoulaz, and R. Iggo.** 2003. Induction of an interferon response by RNAi vectors in mammalian cells. Nat. Genet. **34**:263–264.

5. **Brummelkamp, T. R., R. Bernard, and R. Agami.** 2002. A system for stable expression of short interfering RNAs in mammalian cells. Science **296:**550–553.
6. **Canman, C. E., D.-S. Lim, K. A. Cimprich, Y. Taya, K. Tamai, K. Sakaguchi, E. Apella, M. B. Kastan, and J. D. Siliciano.** 1998. Activation of the ATM kinase by ionizing radiation and phosphorylation of p53. Science **281:**1677–1679.
7. **Cheng, G., J. Zhong, J. Chung, and F. V. Chisari.** 2007. Double-stranded DNA and double-stranded RNA induces a common antiviral signaling pathway in human cells. Proc. Natl. Acad. Sci. USA **104:**9035–9040.
8. **Dansako, H., M. Ikeda, and N. Kato.** 2007. Limited suppression of the interferon-beta production by hepatitis C virus serine protease in cultured human hepatocytes. FEBS J. **274:**4161–4176.
9. **Gaspar, M., and T. Shenk.** 2006. Human cytomegalovirus inhibits a DNA damage response by mislocalizing checkpoint proteins. Proc. Natl. Acad. Sci. USA **103:**2821–2826.
10. **Harper, J. W., and S. J. Elledge.** 2007. The DNA damage response: ten years after. Mol. Cell **28:**739–745.
11. **Ikeda, M., K. Abe, H. Dansako, T. Nakamura, K. Naka, and N. Kato.** 2005. Efficient replication of a full-length hepatitis C virus genome, strain O, in cell culture, and development of a luciferase reporter system. Biochem. Biophys. Res. Commun. **329:**1350–1359.
12. **Kato, N., M. Hijikata, Y. Ootsuyama, M. Nakagawa, S. Ohkoshi, T. Sugimura, and K. Shimotohno.** 1990. Molecular cloning of the human hepatitis C virus genome from Japanese patients with non-A, non-B hepatitis. Proc. Natl. Acad. Sci. USA **87:**9524–9528.
13. **Kato, N.** 2001. Molecular virology of hepatitis C virus. Acta Med. Okayama **55:**133–159.
14. **Kato, N., K. Sugiyama, K. Namba, H. Dansako, T. Nakamura, M. Takami, K. Naka, A. Nozaki, and K. Shimotohno.** 2003. Establishment of a hepatitis C virus subgenomic replicon derived from human hepatocytes infected in vitro. Biochem. Biophys. Res. Commun. **306:**756–766.
15. **Lai, C. K., K. S. Jeng, K. Machida, Y. S. Cheng, and M. M. Lai.** 2008. Hepatitis C virus NS3/4A protein interacts with ATM, impairs DNA repair and enhances sensitivity to ionizing radiation. Virology **370:**295–309.
16. **Lau, A., K. M. Swinbank, P. S. Ahmed, D. L. Taylor, S. P. Jackson, G. C. Smith, and M. J. O'Connor.** 2005. Suppression of HIV-1 infection by a small molecule inhibitor of the ATM kinase. Nat. Cell Biol. **7:**493–500.
17. **Lilley, C. E., R. A. Schwartz, and M. D. Weitzman.** 2007. Using or abusing: viruses and the cellular DNA damage response. Trends Microbiol. **15:**119–126.
18. **Machida, K., K. T. Cheng, V. M. Sung, S. Shimodaira, K. L. Lindsay, A. M. Levine, M. Y. Lai, and M. M. Lai.** 2004. Hepatitis C virus induces a mutator phenotype: enhanced mutations of immunoglobulin and protooncogenes. Proc. Natl. Acad. Sci. USA **101:**4262–4267.
19. **Machida, K., K. T. Cheng, V. M. Sung, K. J. Lee, A. M. Levine, and M. M. Lai.** 2004. Hepatitis C virus infection activates the immunologic (type II) isoform of nitric oxide synthase and thereby enhances DNA damage and mutations of cellular genes. J. Virol. **78:**8835–8843.
20. **Matsuoka, S., M. Huang, and S. J. Elledge.** 1998. Linkage of ATM to cell cycle regulation by the Chk2 protein kinase. Science **282:**1893–1897.
21. **Matsuoka, S., G. Rotman, A. Ogawa, Y. Shiloh, K. Tamai, and S. J. Elledge.** 2000. Ataxia telangiectasia-mutated phosphorylates Chk2 in vivo and in vitro. Proc. Natl. Acad. Sci. USA **97:**10389–10394.
22. **Myong, S., M. M. Bruno, A. M. Pyle, and T. Ha.** 2007. Spring-loaded mechanism of DNA unwinding by hepatitis C virus NS3 helicase. Science **317:**513–516.
23. **Naka, K., H. Dansako, N. Kobayashi, M. Ikeda, and N. Kato.** 2006. Hepatitis C virus NS5B delays cell cycle progression by inducing interferon-β via Toll-like receptor 3 signaling pathway without replicating viral genomes. Virology **346:**348–362.
24. **Naldini, L., U. Blömer, P. Gallay, D. Ory, R. Mulligan, F. H. Gage, I. M. Verma, and D. Trono.** 1996. In vivo gene delivery and stable transduction of nondividing cells by a lentiviral vector. Science **272:**263–267.
25. **Pang, P. S., E. Jankowsky, P. J. Planet, and A. M. Pyle.** 2002. The hepatitis C viral NS3 protein is a processive DNA helicase with cofactor enhanced RNA unwinding. EMBO J. **21:**1168–1176.
26. **Takaoka, A., Z. Wang, M. K. Choi, H. Yanai, H. Negishi, T. Ban, Y. Lu, M. Miyagishi, T. Kodama, K. Honda, Y. Ohba, and T. Taniguchi.** 2007. DAI (DLM-1/ZBP1) is a cytosolic DNA sensor and an activator of innate immune response. Nature **448:**501–505.
27. **Tanaka, T., N. Kato, M. J. Cho, and K. Shimotohno.** 1995. A novel sequence found at the 3′ terminus of hepatitis C virus genome. Biochem. Biophys. Res. Commun. **215:**744–749.
28. **Thomas, D. L.** 2000. Hepatitis C epidemiology. Curr. Top. Microbiol. Immunol. **242:**25–41.
29. **Wakita, T., T. Pietschmann, T. Kato, T. Date, M. Miyamoto, Z. Zhao, K. Murthy, A. Habermann, H. G. Kräusslich, M. Mizokami, R. Bartenschlager, and T. J. Liang.** 2005. Production of infectious hepatitis C virus in tissue culture from a cloned viral genome. Nat. Med. **11:**791–796.
30. **Zufferey, R., D. Nagy, R. J. Mandel, L. Naldini, and D. Trono.** 1997. Multiply attenuated lentiviral vector achieves efficient gene delivery in vivo. Nat. Biotechnol. **15:**871–875.

Biochemical and Biophysical Research Communications 371 (2008) 104–109

Contents lists available at ScienceDirect

Biochemical and Biophysical Research Communications

journal homepage: www.elsevier.com/locate/ybbrc

New efficient replication system with hepatitis C virus genome derived from a patient with acute hepatitis C ☆

Kyoko Mori, Ken-ichi Abe, Hiromichi Dansako, Yasuo Ariumi, Masanori Ikeda, Nobuyuki Kato *

Department of Molecular Biology, Okayama University Graduate School of Medicine, Dentistry, and Pharmaceutical Sciences, 2-5-1 Shikata-cho, Okayama 700-8558, Japan

ARTICLE INFO

Article history:
Received 25 March 2008
Available online 10 April 2008

Keywords:
Hepatitis C virus
Acute hepatitis C
HCV replication system
Genome-length HCV RNA
Anti-HCV reagents
Interferon-γ

ABSTRACT

We report for the first time a new RNA replication system with a hepatitis C virus (HCV) strain (AH1) derived from a patient with acute hepatitis C. Using an HCV replicon RNA library constructed with the AH1 strain (genotype 1b), we first established a cloned cell line, sAH1, harboring the HCV replicon. Cured cells obtained with interferon treatment of sAH1 cells were used for transfection with genome-length HCV RNA possessing four mutations found in sAH1 replicon. Consequently, one cloned cell line, AH1, supporting efficient replication of genome-length HCV RNA was obtained. By the comparison of AH1 cells with the O cells supporting genome-length HCV RNA (HCV-O strain) replication, we found different anti-HCV profiles of interferon-γ and cyclosporine A between AH1 and O cells. Reporter assay analysis suggests that the diverse effects of interferon-γ are due to the difference in HCV strains, but not the cellular environment.

Hepatitis C virus (HCV) infection frequently causes chronic hepatitis, which progresses to liver cirrhosis and hepatocellular carcinoma. HCV infection has now become a serious health problem because at least 170 million people worldwide are currently infected with HCV [1]. HCV is an enveloped virus with a positive single-stranded 9.6 kilobase (kb) RNA genome, which encodes a large polyprotein precursor of approximately 3000 amino acid (aa) residues [2,3]. This polyprotein is cleaved by a combination of the host and viral proteases into at least 10 proteins in the following order: core, envelope 1 (E1), E2, p7, non-structural 2 (NS2), NS3, NS4A, NS4B, NS5A, and NS5B [3].

As a striking breakthrough in HCV research, in 1999, an HCV replicon system enabling robust HCV subgenomic RNA (Con-1 strain of genotype 1b) replication in specific human HuH-7 hepatoma cells has been developed [4]. After the first Con-1 replicon, several HCV replicon (genotypes 1a, 1b, and 2a) systems using HuH-7-derived cells have been developed. These replicon systems have become powerful tools for basic studies of HCV replication, HCV–host cell interactions, and screening of anti-HCV reagents, [5,6]. Furthermore, genome-length HCV RNA replication systems have been developed [7–9], since HCV replicons lacking HCV structural proteins are insufficient for further HCV research. We also established a genome-length HCV RNA-replicating cell line (HCV-O strain of genotype 1b; called O cell line) [10] using cured cells derived from sO cells [11], in which HCV replicon RNA (HCV-O strain) with an adaptive mutation (S2200R) is replicating. However, to date, established genome-length HCV RNA-replicating stable cell lines are limited to five HCV strains, H77 (1a), HCV-N (1b), Con-1 (1b), HCV-O (1b), and JFH1 (2a) [7–10,12], and there is no RNA replication system with an HCV strain derived from a patient with acute hepatitis C. Furthermore, there have been few reports comparing these HCV strains.

To clarify these problems, we have attempted to establish a new stable cell line, in which genome-length HCV RNA derived from a patient with acute hepatitis C is efficiently replicating. We report herein a new efficient RNA replication system with HCV derived from a patient with acute hepatitis C and provide a comparative analysis of RNA replication systems with AH1 and HCV-O strains regarding the sensitivities to anti-HCV reagents, including interferon (IFN)-α.

Materials and methods

Cell culture. Cells supporting HCV replicon or genome-length HCV RNA, and cured cells, from which the HCV RNA had been eliminated by IFN treatment, were maintained as described previously [10].

Reverse transcription (RT)-nested PCR. RNA from a serum of patient AH1 [13] with acute hepatitis C was prepared using the ISOGEN-LS extraction kit (Nippon Gene Co., Japan). This RNA sample was used as a template for RT-nested PCR to amplify the HCV RNA. RT-nested PCR was performed separately in two parts; one part (3.5 kb) covered from HCV 5′UTR to NS3, and the other part (6 kb) covered from NS2 to NS5B. For the first part, the antisense primer AH3553R, 5′-CACACGCCGTTGATGC AGGTCG-3′ was used for RT. Primers 21 [11] and AH3519R, 5′-TGCGTGGCGG

☆ The nucleotide sequence data reported in this paper will appear in the DDBJ, EMBL, and GenBank nucleotide sequence databases under Accession No. AB429050.

* Corresponding author. Fax: +81 86 235 7392.
E-mail address: nkato@md.okayama-u.ac.jp (N. Kato).

0006-291X/$ - see front matter © 2008 Elsevier Inc. All rights reserved.
doi:10.1016/j.bbrc.2008.04.005

TGGAAACCACCTG-3′ were employed in the first round of PCR (35 cycles). An internal primer pair (21X [11] and AH3466RX: 5′-ATTATTCTAGAGGCCTGTGAGACTG GTGATGATGC-3′; containing a XbaI site (underlined)) was used for the second round of PCR (35 cycles). For the second part, the antisense primer 386R [11] was used for RT. Primers 542 and 9388R [11] were employed in the first round of PCR (35 cycles). An internal primer pair (3295X: 5′-ATTATTCTAGACTGACATGGA GACCAAGATCATCAC-3′; containing a XbaI site (underlined) and 9357RX: 5′-ATTATT CTAGACCCGTTCACCGGTTGGGGAGCAG-3′; containing a XbaI site (underlined)) was used for the second round of PCR (35 cycles). These fragments overlapped at the NS2 and NS3 regions and were used for sequence analysis for HCV RNA after cloning into the XbaI site of pBR322MC [11]. Superscript II (Invitrogen) and KOD-plus DNA polymerase (Toyobo, Osaka, Japan) were used for RT and PCR, respectively.

Plasmid construction. PCR product (NS3 to NS5B of AH1 strain) with primers 542 and 9388R was further amplified with primers 3501S: 5′-ATTATACTAGTCTCACAGG CCGGGACAAGAACC-3′; containing a SpeI site (underlined) and 9162RB: 5′-ATTATC GTACGGCCCAGTTGAAGAGGTACTTGCC-3′; containing a BsiWI site (underlined). The amplified fragment was digested with SpeI and BsiWI, and ligated into the replicon cassette plasmid pNSS1RZ2RU [11], which was predigested with SpeI and BsiWI. Using this ligation reaction mixture, a replicon RNA library (AH1N/3-5B in Supplementary Fig. 1) was prepared by a previously described method [11]. To make the plasmid pAH1N/C-5B/PL, LS, $(VA)_2$ containing full-length HCV polyprotein of AH1 strain, pON/C-5B containing full-length HCV polyprotein of HCV-O strain [10] was utilized. First, to make a fragment for pAH1N/C-5B (Supplementary Fig. 1), overlapping PCR was used to fuse EMCV IRES to the core protein-coding sequence of the AH1 strain, as described previously [10]. The resulting DNA was digested with PmeI and ClaI, and then replaced with the PmeI–ClaI fragment of pON/C-5B (pON/C-5B/CoreAH was obtained). Second, the ClaI–AgeI fragment of pHCV-AH1 containing full-length HCV polyprotein of AH1 strain was replaced with the ClaI–AgeI fragment of pON/C-5B/CoreAH (pAH1N/C-5B was obtained). Finally, the SpeI–BsiWI fragment of pAH1N/3-5B clone 2 (see Fig. 1C) was replaced with the SpeI–BsiWI fragment of pAH1N/C-5B (pAH1N/C-5B/PL, LS, $(VA)_2$ was obtained).

RNA synthesis. Plasmid DNAs were linearized by XbaI and were used for RNA synthesis with T7 MEGAscript (Ambion) as previously described [11].

RNA transfection and selection of G418-resistant cells. The transfection of HCV replicon RNA or genome-length HCV RNA synthesized in vitro into HuH-7-derived cells was performed by electroporation, and the cells were selected in the presence of G418 (0.3 mg/ml; Promega) for 3 weeks as described previously [11].

Quantification of HCV RNA. The quantitative RT-PCR (RT-qPCR) analysis for HCV RNA was performed by LightCycler PCR as described previously [10]. Experiments were done in triplicate.

Integration analysis. Genomic DNA was extracted from the cultured cells using the DNeasy Blood & Tissue Kit (QIAGEN). The HCV 5′UTR and the IFN-β gene were detected according to a PCR method described previously [11].

Western blot analysis. The preparation of cell lysates, sodium dodecyl sulfate–polyacrylamide gel electrophoresis, and immunoblotting analysis were performed as previously described [11]. The antibodies used in this study were those against Core, E2, NS3, NS4A, NS5A, and NS5B [10]. β-Actin antibody (AC-15, Sigma) was used as the control for the amount of protein loaded per lane. Immunocomplexes were detected with the Renaissance enhanced chemiluminescence assay (Perkin-Elmer Life Sciences, Boston, MA).

Sequence analysis of HCV RNA. To amplify replicon RNA and genome-length HCV RNA, RT-PCR was performed as described previously [10,11]. The PCR products were subcloned into the XbaI site of pBR322MC, and sequence analysis was performed as described previously [11].

Northern blot analysis. Total RNA was extracted from the cultured cells using the RNeasy Mini Kit (QIAGEN). Three micrograms of total RNA was used for the analysis. HCV-specific RNA and β-actin were detected according to a method described previously [10].

Luciferase reporter assay. For the dual-luciferase assay, firefly luciferase vectors, pGBP-1(-216)-Luc and p2′–5′-OAS(-159)-Luc [14], were used. The reporter assay was performed as previously described [14]. The experiments were performed in at least triplicate.

Statistical analysis. Differences between AH1 and O cell lines were tested using the Student's *t*-test. *P* values <.05 were considered statistically significant.

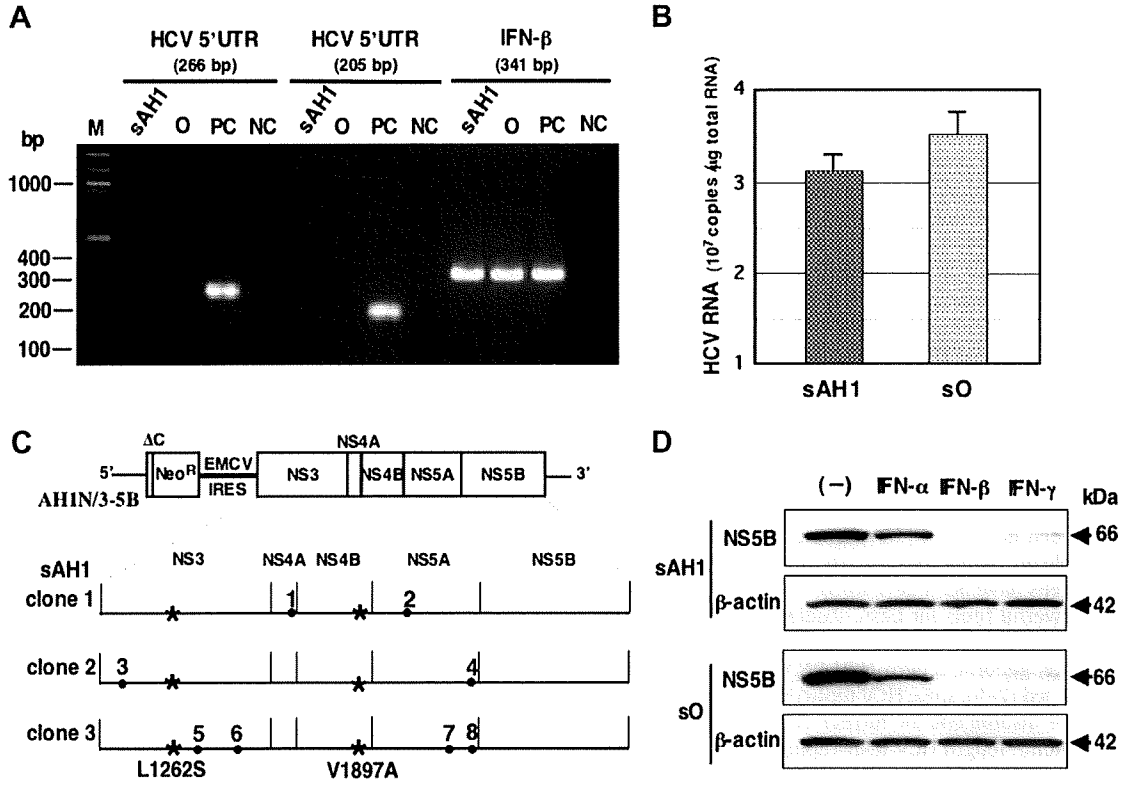

Fig. 1. Characterization of sAH1 cells harboring HCV replicon. (A) No integration of the HCV sequence in the genomic DNA. Genomic DNA from sAH1cells was subjected to PCR for the detection of the HCV 5′UTR and the IFN-β gene. O cells were used as a negative control. Lane PC, HCV sequence-integrated cells; lane NC, no genomic DNA; lane M, 100 bp DNA ladder. PCR products were detected by staining with ethidium bromide after 3% agarose gel electrophoresis. (B) Quantitative analysis of intracellular replicon RNA. The levels of replicon RNA were quantified by LightCycler PCR. sO cells harboring HCV-O replicon [11] were used for the comparison. (C) Amino acid substitutions detected in intracellular AH1 replicon RNA. NS3 to NS5B regions of three independent clones sequenced were presented. L1262S and V1897A conserved substitutions are indicated by asterisks. Clone-specific aa substitutions (indicated by the numbers with dots) are as follows: 1, K1691R; 2, M2105I; 3, P1115L; 4, V2360A; 5, K1368R; 6, A1533T; 7, I2285V; 8, D2377H. (D) IFN sensitivity of AH1 replicon. sAH1 cells were treated with IFN-α (Sigma), IFN-β (a gift from Toray Industries), and IFN-γ (Sigma) (20 IU/ml each) for 5 days. For the comparison, sO cells were treated as well as sAH1 cells. NS5B was detected by Western blot analysis.

Results

Establishment of a G418-resistant cell line (sAH1) harboring HCV replicon RNA

An HCV replicon RNA library prepared from the AH1 strain was first transfected into sOc cells (cured sO cells) [11], and the G418-resistant cells were selected as described previously [11]. Although several G418-resistant colonies were obtained, production of these colonies was due to integration of the HCV RNA sequence into the chromosomal DNA (PC in Fig. 1A). Therefore, we further cleaned up the replicon RNA library with additional DNase treatment, and it was then transfected into OR6c cells (cured OR6 cells) [10]. Consequently, a G418-resistant colony was obtained and successfully proliferated; this colony was referred to as sAH1. To exclude the possibility of integration of a replicon RNA sequence into the genomic DNA, we examined the presence of the HCV 5′UTR sequence in the genomic DNA isolated from sAH1 cells by a PCR method described previously [11]. Genome-length HCV RNA-replicating O cells were also examined as a negative control. The results revealed that the HCV RNA sequence was not integrated into the genomic DNA in either sAH1 cells or O cells (Fig. 1A).

Regarding the level of replicon RNA in sAH1 cells, RT-qPCR analysis revealed that the titer of replicon RNA was approximately 3×10^7 copies/μg total RNA, and its level was equivalent to that in sO cells (Fig. 1B), suggesting that the efficiency of RNA replication in sAH1 cells is similar to that in sO cells.

To exclude the possibility that sAH1 cells were derived from a small number of OR6 cells remaining after IFN treatment, and to determine whether replicon RNA in sAH1 cells possesses cell culture-adaptive mutations [5], which enhance the efficiency of RNA replication, we performed genetic analysis of the intracellular AH1 replicon. The sequences of three independent clones were determined and compared with each other to avoid PCR error. The obtained consensus nucleotide and aa sequences of NS3–NS5B regions of the AH1 replicon showed 7.3% and 3.7% differences, respectively, from those of the HCV-O replicon [11], indicating that sAH1 cells were not contaminated by the OR6 cells. In contrast, to find conserved mutations in the AH1 replicon, we determined the consensus nucleotide sequences of AH1 serum-derived HCV RNA by comparison of the nucleotide sequences of three independently isolated cDNA clones (Accession No. AB429050). The K1609E (NS3) and S2200R (NS5A) adaptive mutations found in O and OR6 cells were not detected in the AH1 replicon. However, instead of these mutations, L1262S (NS3) and V1897A (NS4B) conserved mutations were detected (Fig. 1C). Although V1897A has been detected as an adaptive mutation in Con-1 replicon [15], L1262S has until now remained undetected. In clone 2, the P1115L mutation (number 3 in Fig. 1C), which has been reported as an adaptive mutation [15,16], was detected.

To further characterize the sAH1 replicon, we compared the sensitivities of sAH1 and sO replicons against anti-HCV reagents (IFN-α, IFN-β, and IFN-γ) [5,6,11]. Western blot analysis of NS5B revealed that the IFN sensitivity of the sAH1 replicon was equivalent to that of the sO replicon (Fig. 1D).

Establishment of a genome-length HCV-AH1 RNA-replicating cell line, AH1

To develop a genome-length HCV RNA replication system, we first constructed a pAH1N/C-5B/PL, LS, $(VA)_2$ by the replacement with sAH1 replicon clone 2 (Fig. 1C) into pAH1N/C-5B. AH1N/C-5B/PL, LS, $(VA)_2$ RNA was transfected into sAH1c cells, cured sAH1 cells. Following 3 weeks of culturing in the presence of

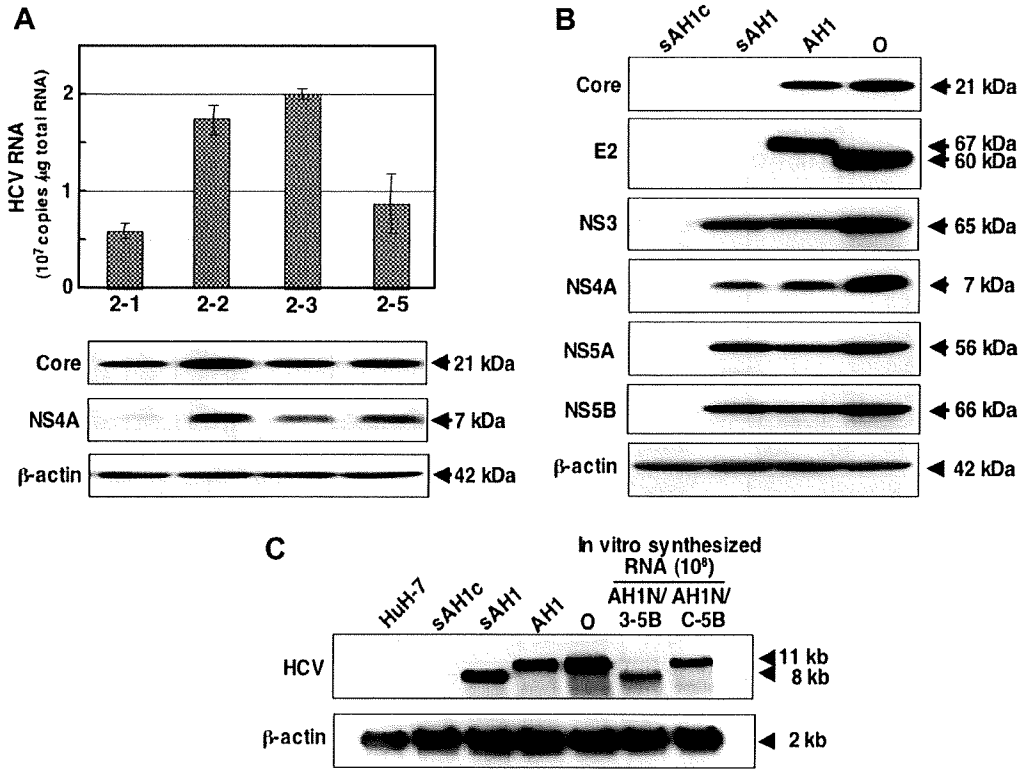

Fig. 2. Characterization of AH1 cells harboring genome-length HCV RNA. (A) Selection of G418-resistant cell lines. The levels of HCV RNA in G418-resistant cells were quantified by LightCycler PCR (upper panel). Core and NS4A were detected by Western blot analysis (lower panel). (B) Western blot analysis. AH1, O, sAH1, and sAH1c cells were used for the comparison. Core, E2, NS3, NS4A, NS5A, and NS5B were detected by Western blot analysis. (C) Northern blot analysis. AH1, O, sAH1, sAH1c, and HuH-7 cells were used for the comparison. In vitro-synthesized AH1N/3-5B and AH1N/C-5B RNAs were also used for the comparison.

G418, several colonies were obtained, and 4 colonies (2-1, 2-2, 2-3, and 2-5) then successfully proliferated. We selected colony 2-2 among them because it showed high levels of HCV RNA and proteins (core and NS4A) (Fig. 2A); this cell line was referred to as AH1. To compare the expression levels of HCV proteins in AH1 cells with those in O cells, Western blot analysis was further performed. Although the levels of HCV proteins in AH1 cells were slightly lower than those in O cells, the expression levels of NS proteins in AH1 cells were equivalent to those in sAH1 cells (Fig. 2B). In this analysis, we noticed that the size of the E2 protein in AH1 cells was 7 kDa larger than that in O cells (Fig. 2B). This difference may be due to the different numbers of *N*-glycosylation sites in E2 protein, since 11 and 9 *N*-glycosylation sites in E2 proteins are estimated in AH1 and HCV-O strains, respectively. Northern blot analysis also showed the presence of HCV-specific RNA with a length of approximately 11 kb in the extracts of total RNA prepared from AH1 cells, similar to that in the O cells (Fig. 2C). We confirmed the presence of replicon RNA (approximately 8 kb) in sAH1 cells (Fig. 2C). To check the additional adaptive mutations in the genome-length AH1 RNA, we performed sequence analysis of HCV RNA in AH1 cells. The results (Supplementary Fig. 2) revealed no additional mutations detected commonly among the three independent clones sequenced, suggesting that additional adaptive mutations are not required for genome-length HCV RNA replication. We therefore conclude that the AH1 cell line can be used as a genome-length HCV RNA replication system with acute hepatitis C-derived HCV strain.

Diverse effects of anti-HCV reagents on HCV RNA replication in AH1 and O cells

To compare the effects of anti-HCV reagents on RNA replication systems with different HCV strains, we examined the anti-HCV profiles of IFN-α, IFN-γ, and cyclosporine A (CsA) [17] using AH1 and O cells. Regarding IFN-α, the anti-HCV effect in AH1 cells was similar to that in O cells (Fig. 3A). Although RT-qPCR analysis showed a statistically significant difference in both cell systems when 1 IU/ml of IFN-α was used, such a difference was not observed in the Western blot analysis (Fig. 3A). In contrast, a significant different effect of IFN-γ was observed in both cell systems. RT-qPCR and Western blot analyses revealed that RNA replication of the AH1 strain was less sensitive than that of the HCV-O strain when 1 or 10 IU/ml of IFN-γ was used (Fig. 3B). Conversely, we observed that RNA replication of the AH1 strain was more sensitive to CsA than that of the HCV-O strain (Fig. 3C). These results suggest that anti-HCV profiles of IFN-γ and CsA are rather different between AH1 and O cell systems.

Different anti-HCV profile of IFN-γ is not correlated with the cellular potentials of the IFN-γ signaling pathway

To clarify whether the different effects of IFN-γ observed between AH1 and O cells are dependent on the cellular potentials of the IFN-γ signaling pathway, we performed a dual-luciferase reporter assay using an IFN-γ-inducible intrinsic GBP-1 gene promoter. As a control, IFN-α-inducible intrinsic 2′–5′-OAS gene promoter was also used for the analysis of the IFN-α signaling pathway. The results revealed that a good response of both AH1 and O cells to IFN-α and IFN-γ stimulation, with their potentials for both signaling pathways being almost the same (Fig. 4). These results suggest that the diverse anti-HCV effects of IFN-γ are dependent on the HCV strain, but not on the cellular potentials of the IFN-γ signaling pathway.

Discussion

In the present study, we established for the first time an HCV RNA replication system with AH1 strain derived from a patient

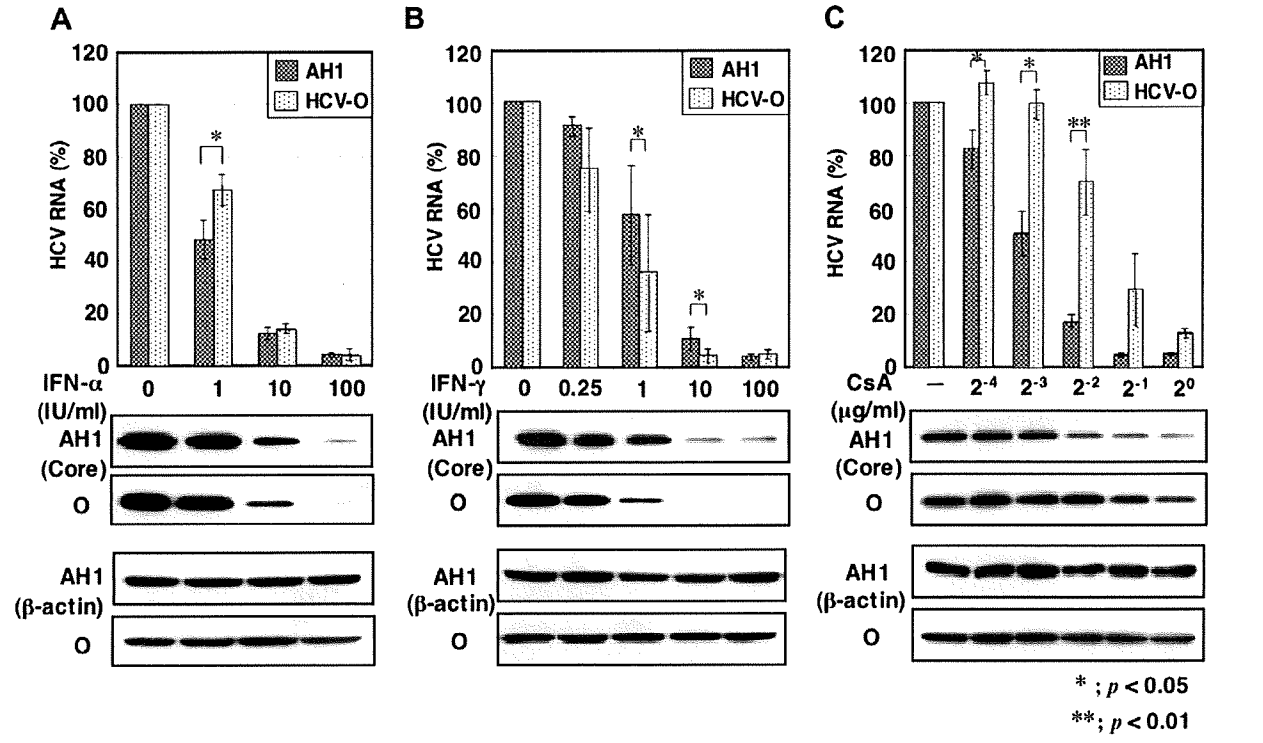

Fig. 3. The diverse effects of anti-HCV reagents on AH1 and HCV-O RNA replications. AH1 and O cells were treated with anti-HCV reagents for 72 h, and then extracted total RNAs and cell lysates were subjected to RT-qPCR for HCV 5′ UTR (each upper panel) and Western blot analysis for the core protein (each lower panel), respectively. (A) Effect of IFN-α. (B) Effect of IFN-γ. (C) Effect of CsA (Sigma).

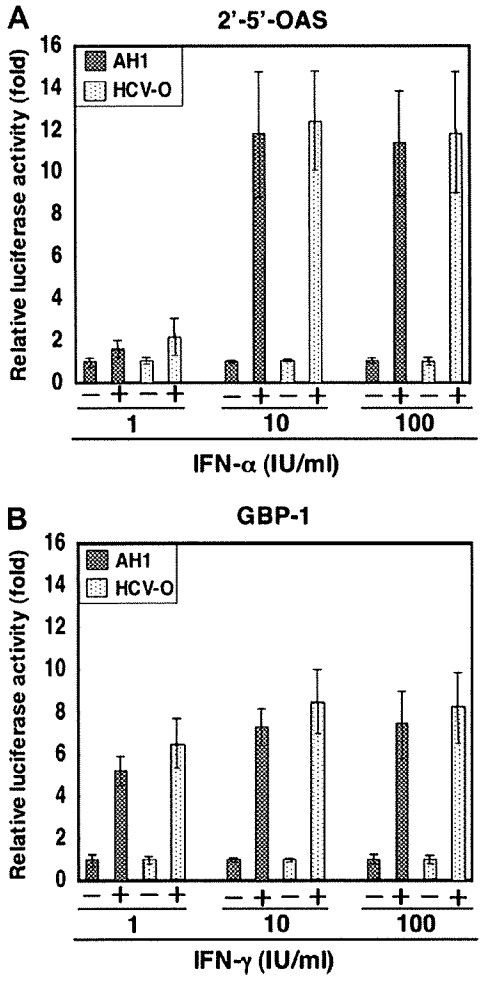

Fig. 4. Dual-luciferase reporter assay of IFN-α or IFN-γ-inducible gene promoter. AH1 and O cells were treated for 6 h with IFN-α or IFN-γ before the reporter assay. (A) 2′–5′-OAS gene promoter. (B) GBP-1 gene promoter.

with acute hepatitis C, and found diverse anti-HCV effects of IFN-γ and CsA between AH1 and HCV-O strains.

The levels of HCV replicon RNA and genome-length HCV RNA in sAH1 and AH1 cells were assigned to 3×10^7 and 2×10^7 copies/μg total RNA, respectively. These values are similar to those obtained from previously established HCV RNA replication systems [5]. Since known adaptive mutations (P1115L and V1897A) and additional conserved mutations (L1262S) were detected in the developed sAH1 replicon, these mutations may contribute to enhanced levels of RNA replication. The expression levels of genome-length HCV RNA and proteins observed in the present study suggest that genome-length HCV RNA replication efficiently occurs in AH1 cells, and that this RNA replication system is useful for comparison with already developed genome-length HCV RNA replication systems with HCV-N [7], Con-1 [8,9], or HCV-O [10] strains.

In the comparative analysis of genome-length HCV RNA replication systems with AH1 and HCV-O strains, we found that IFN-γ and CsA showed different anti-HCV profiles between AH1 and HCV-O strains. Regarding IFN-γ, RNA replication of the AH1 strain (EC_{50} = 1.9 IU/ml) was less sensitive than that of the HCV-O strain (EC_{50} = 0.3 IU/ml). Windisch et al. [18] have previously reported that RNA replication in an HCV replicon system using HuH-6 hepatoma cells is highly resistant (EC_{50} was more than 100 IU/ml) to IFN-γ, and that its resistant phenotype is not due to a general defect in the IFN-γ signaling pathway. In that study, they speculated that some mutations within a critical effector gene in HuH-6 cells might account for the inability of the cells to reduce the number of replicon RNAs in response to IFN-γ. Although such a possibility is not completely excluded, the diverse effects of IFN-γ observed in the present study were likely due to the difference in viral strains because RNA replication of the AH1 strain is still sensitive to IFN-γ. To clarify this point, development of an additional HCV RNA replication system such as an OR6 assay system with more quantitative reporter genes [10] is needed.

Regarding CsA, RNA replication of the AH1 strain (EC_{50} = 0.13 μg/ml) showed more sensitivity than that of the HCV-O strain (EC_{50} = 0.35 μg/ml). Ishii et al. [17] have previously reported that RNA replication of the JFH1 strain (genotype 2a) is less sensitive to CsA than genotype 1b strains, including the HCV-O strain. In that study, they concluded that the difference in sensitivity of JFH1 and genotype 1b strains to CsA could be attributed to characteristic differences in the HCV strains, not to the parent cell strain. In addition, sensitivity to CsA was almost the same among genotype 1b strains in that study. Therefore, we estimate that the AH1 strain is more sensitive to CsA than these genotype 1b strains examined to date. Further analysis will be necessary to clarify the mechanism underlying differences in sensitivity to CsA among genotype 1b strains.

In conclusion, an HCV RNA replication system with the AH1 strain would be useful for comparison with other strain-derived systems in various HCV studies, including analysis of the effects of anti-HCV reagents.

Acknowledgments

We thank T. Nakamura for technical assistance. We also thank A. Takamizawa and M. Kohara for the anti-NS3, NS4A, NS5A, and NS5B antibodies. This work was supported by grants-in-aid for a third-term comprehensive 10-year strategy for cancer control, and for research on hepatitis from the Ministry of Health, Labor, and Welfare of Japan.

Appendix A. Supplementary data

Supplementary data associated with this article can be found, in the online version, at doi:10.1016/j.bbrc.2008.04.005.

References

[1] D.L. Thomas, Hepatitis C epidemiology, Curr. Top. Microbiol. Immunol. 242 (2000) 25–41.
[2] N. Kato, M. Hijikata, Y. Ootsuyama, M. Nakagawa, S. Ohkoshi, T. Sugimurd, K. Sugimurd, Molecular cloning of the human hepatitis C virus genome from Japanese patients with non-A, non-B hepatitis, Proc. Natl. Acad. Sci. USA 87 (1990) 9524–9528.
[3] N. Kato, Molecular virology of hepatitis C virus, Acta Med. Okayama 55 (2001) 133–159.
[4] V. Lohmann, F. Korner, J. Koch, U. Herian, L. Theilmann, R. Bartenschlager, Replication of subgenomic hepatitis C virus RNAs in a hepatoma cell line, Science 285 (1999) 110–113.
[5] R. Bartenschlager, S. Sparacio, Hepatitis C virus molecular clones and their replication capacity in vivo and in cell culture, Virus Res. 127 (2007) 195–207.
[6] J.M. Pawlotsky, S. Chevaliez, J.G. McHutchison, The hepatitis C virus life cycle as a target for new antiviral therapies, Gastroenterology 132 (2007) 1979–1998.
[7] M. Ikeda, M. Yi, K. Li, S.M. Lemon, Selectable subgenomic and genome-length dicistronic RNAs derived from an infectious molecular clone of the HCV-N strain of hepatitis C virus replicate efficiently in cultured Huh7 cells, J. Virol. 76 (2002) 2997–3006.
[8] T. Pietschmann, V. Lohmann, A. Kaul, N. Krieger, G. Rinck, G. Rutter, D. Strand, R. Bartenschlager, Persistent and transient replication of full-length hepatitis C virus genomes in cell culture, J. Virol. 76 (2002) 4008–4021.
[9] K.J. Blight, J.A. McKeating, J. Marcotrigiano, C.M. Rice, Efficient replication of hepatitis C virus genotype 1a RNAs in cell culture, J. Virol. 77 (2003) 3181–3190.

[10] M. Ikeda, K. Abe, H. Dansako, T. Nakamura, K. Naka, N. Kato, Efficient replication of a full-length hepatitis C virus genome, strain O, in cell culture, and development of a luciferase reporter system, Biochem. Biophys. Res. Commun. 329 (2005) 1350–1359.
[11] N. Kato, K. Sugiyama, K. Namba, H. Dansako, T. Nakamura, M. Takami, K. Naka, A. Nozaki, K. Shimotohno, Establishment of a hepatitis C virus subgenomic replicon derived from human hepatocytes infected in vitro, Biochem. Biophys. Res. Commun. 306 (2003) 756–766.
[12] T. Wakita, T. Pietschmann, T. Kato, T. Date, M. Miyamoto, Z. Zhao, K. Murthy, A. Habermann, H.G. Krausslich, M. Mizokami, R. Bartenschlager, T.J. Liang, Production of infectious hepatitis C virus in tissue culture from a cloned viral genome, Nat. Med. 11 (2005) 791–796.
[13] N. Kato, H. Sekiya, Y. Ootsuyama, T. Nakazawa, M. Hijikata, S. Ohkoshi, K. Shimotohno, Humoral immune response to hypervariable region 1 of the putative envelope glycoprotein (gp70) of hepatitis C virus, J. Virol. 67 (1993) 3923–3930.
[14] H. Dansako, A. Naganuma, T. Nakamura, F. Ikeda, A. Nozaki, N. Kato, Differential activation of interferon-inducible genes by hepatitis C virus core protein mediated by the interferon stimulated response element, Virus Res. 97 (2003) 17–30.
[15] V. Lohmann, S. Hoffmann, U. Herian, F. Penin, R. Bartenschlager, Viral and cellular determinants of hepatitis C virus RNA replication in cell culture, J. Virol. 77 (2003) 3007–3019.
[16] K. Abe, M. Ikeda, H. Dansako, K. Naka, N. Kato, Cell culture-adaptive NS3 mutations required for the robust replication of genome-length hepatitis C virus RNA, Virus Res. 125 (2007) 88–97.
[17] N. Ishii, K. Watashi, T. Hishiki, K. Goto, D. Inoue, M. Hijikata, T. Wakita, N. Kato, K. Shimotohno, Diverse effects of cyclosporine on hepatitis C virus strain replication, J. Virol. 80 (2006) 4510–4520.
[18] MP. Windisch, M. Frese, A. Kaul, M. Trippler, V. Lohmann, R. Bartenschlager, Dissecting the interferon-induced inhibition of hepatitis C virus replication by using a novel host cell line, J. Virol. 79 (2005) 13778–13793.

JOURNAL OF VIROLOGY, Mar. 2009, p. 2338–2348 Vol. 83, No. 5
0022-538X/09/$08.00+0 doi:10.1128/JVI.01840-08

Arsenic Trioxide Inhibits Hepatitis C Virus RNA Replication through Modulation of the Glutathione Redox System and Oxidative Stress[▽]

Misao Kuroki,[1] Yasuo Ariumi,[1] Masanori Ikeda,[1] Hiromichi Dansako,[1] Takaji Wakita,[2] and Nobuyuki Kato[1]*

Department of Tumor Virology, Okayama University Graduate School of Medicine, Dentistry, and Pharmaceutical Sciences, 2-5-1, Shikata-cho, Okayama 700-8558, Japan,[1] and Department of Virology II, National Institute of Infectious Diseases, 1-23-1 Toyama, Shinjuku-ku, Tokyo 162-8640, Japan[2]

Received 2 September 2008/Accepted 13 December 2008

Arsenic trioxide (ATO), a therapeutic reagent used for the treatment of acute promyelocytic leukemia, has recently been reported to increase human immunodeficiency virus type 1 infectivity. However, in this study, we have demonstrated that replication of genome-length hepatitis C virus (HCV) RNA (O strain of genotype 1b) was notably inhibited by ATO at submicromolar concentrations without cell toxicity. RNA replication of HCV-JFH1 (genotype 2a) and the release of core protein into the culture supernatants were also inhibited by ATO after the HCV infection. To clarify the mechanism of the anti-HCV activity of ATO, we examined whether or not PML is associated with this anti-HCV activity, since PML is known to be a target of ATO. Interestingly, we observed the cytoplasmic translocation of PML after treatment with ATO. However, ATO still inhibited the HCV RNA replication even in the PML knockdown cells, suggesting that PML is dispensable for the anti-HCV activity of ATO. In contrast, we found that *N*-acetyl-cysteine, an antioxidant and glutathione precursor, completely and partially eliminated the anti-HCV activity of ATO after 24 h and 72 h of treatment, respectively. In this context, it is worth noting that we found an elevation of intracellular superoxide anion radical, but not hydrogen peroxide, and the depletion of intracellular glutathione in the ATO-treated cells. Taken together, these findings suggest that ATO inhibits the HCV RNA replication through modulation of the glutathione redox system and oxidative stress.

Hepatitis C virus (HCV) is the causative agent of chronic hepatitis, which progresses to liver cirrhosis and hepatocellular carcinoma. HCV is an enveloped virus with a positive single-stranded 9.6-kb RNA genome, which encodes a large polyprotein precursor of approximately 3,000 amino acid residues. This polyprotein is cleaved by a combination of the host and viral proteases into at least 10 proteins in the following order: core, envelope 1 (E1), E2, p7, nonstructural 2 (NS2), NS3, NS4A, NS4B, NS5A, and NS5B (30).

Alpha interferon has been used as an effective anti-HCV reagent in clinical therapy for patients with chronic hepatitis C. The current combination treatment with pegylated alpha interferon and ribavirin, a nucleoside analogue, has been shown to improve the sustained virological response rate to more than 50% (15). However, the adverse effects of the combination therapy and the limited efficacy against genotype 1b warrant the development of new anti-HCV reagents.

Arsenic trioxide (ATO) (As_2O_3, arsenite) has been used as a therapeutic reagent in acute promyelocytic leukemia, which bears an oncogenic PML-retinoic acid receptor alpha fusion protein resulting from chromosomal translocation (51, 52, 68, 70). The ATO treatment induces complete remission through degradation of the aberrant PML-retinoic acid receptor α (70). The PML tumor suppressor protein is required for formation of the PML nuclear body (PML-NB), also known as nuclear dot 10 or the PML oncogenic domain, which is often disrupted by infection with DNA viruses, such as herpes simplex virus type 1, human cytomegalovirus, and Epstein-Barr virus (17). The treatment with ATO results in degradation of the PML protein and disruption of the PML-NB (70). Therefore, ATO has been become a useful probe for investigating the functions of the PML-NB, including cell growth, apoptosis, stress response, and viral infection. Indeed, ATO has been shown to increase retroviral infectivity, such as human immunodeficiency virus type 1 (HIV-1) and murine leukemia virus infectivity, but the mechanisms of this change are not well understood (5, 6, 32, 44, 47, 50, 57). In contrast, ATO was recently reported to inhibit the replication of HCV subgenomic replicon RNA (24). However, it also remains unclear how ATO inhibits the HCV RNA replication. In this study, using genome-length HCV RNA replication systems, we investigated the molecular mechanism(s) of the anti-HCV activity of ATO, and we provide evidence that ATO inhibits HCV RNA replication through modulation of the glutathione redox system and oxidative stress.

MATERIALS AND METHODS

Reagents. ATO, *N*-acetyl-cysteine (NAC), ascorbic acid (vitamin C), and L-buthionine sulfoximine (BSO) were purchased from Sigma (St. Louis, MO). Arsenic pentoxide (APO) (As_2O_5, arsenate) was purchased from Wako (Osaka, Japan). Both ATO and APO were dissolved in 1 N NaOH at 0.1 M as a stock solution. An inducible nitric oxide synthase (iNOS) inhibitor, 1400W, was purchased from Calbiochem (Merck Biosciences, Darmstadt, Germany).

Cell culture. 293FT cells were cultured in Dulbecco's modified Eagle's medium (Invitrogen, Carlsbad, CA, USA) supplemented with 10% fetal bovine serum. The following four HuH-7-derived cell lines or their parental HuH-7 cells

* Corresponding author. Mailing address: Department of Tumor Virology, Okayama University Graduate School of Medicine, Dentistry, and Pharmaceutical Sciences, 2-5-1, Shikata-cho, Okayama 700-8558, Japan. Phone: 81 86 235 7385. Fax: 81 86 235 7392. E-mail: nkato@md.okayama-u.ac.jp.

▽ Published ahead of print on 24 December 2008.

were cultured in Dulbecco's modified Eagle's medium with 10% fetal bovine serum as described previously (25): O cells, harboring a replicative genome-length HCV-O RNA (O strain of genotype 1b) (25); OR6 cells, harboring the genome-length HCV-O RNA with luciferase as a reporter (25); sO cells, harboring the subgenomic replicon RNA of HCV-O (31); and RSc cured cells, which cell culture-generated HCV-JFH1 (JFH1 strain of genotype 2a) (58) could infect and effectively replicate in (2, 3). The O, OR6, and sO cells were maintained in the presence of G418 (300 μg/ml Geneticin; Invitrogen).

RNA interference. Oligonucleotides with the following sense and antisense sequences were used for the cloning of short hairpin RNA (shRNA)-encoding sequences targeted to PML (56) in a lentiviral vector: 5′-GATCCCCAGATGC AGCTGTATCCAAGTTCAAGAGACTTGGATACAGCTGCATCTTTTTTG GAAA-3′ (sense) and 5′-AGCTTTTCCAAAAAAGATGCAGCTGTATCCAA GTCTCTTGAACTTGGATACAGCTGCATCTGGG-3′ (antisense). These oligonucleotides were annealed and subcloned into the BglII-HindIII site, downstream from an RNA polymerase III promoter of pSUPER (8), to generate pSUPER-PMLi. To construct pLV-PMLi, the BamHI-SalI fragments of pSUPER-PMLi were subcloned into the BamHI-SalI site of pRDI292, an HIV-1-derived self-inactivating lentiviral vector containing a puromycin resistance marker allowing for the selection of transduced cells (7). pLV-Chk2i was described previously (3).

Lentiviral vector production. The vesicular stomatitis virus (VSV) G-pseudotyped HIV-1-based vector system has been described previously (42). The lentiviral vector particles were produced by transient transfection of the second-generation packaging construct pCMV-ΔR8.91 (1, 71) and the VSV G envelope-expressing plasmid pMDG2 as well as pRDI292 into 293FT cells with FuGene6 (Roche Diagnostics, Mannheim, Germany).

HCV infection experiments. The supernatants was collected from cell culture-generated HCV-JFH1 (58)-infected RSc cells (2, 3) at 5 days postinfection and stored at −80°C after filtering through a 0.45-μm filter (Kurabo, Osaka, Japan) until use. For infection experiments with HCV-JFH1 virus, RSc cells (1×10^5 cells/well) were plated onto six-well plates and cultured for 24 h. We then infected the cells with 50 μl (equivalent to a multiplicity of infection of 0.05 to 0.1) of inoculum. The culture supernatants were collected at 97 h postinfection, and the levels of the core protein were determined by enzyme-linked immunosorbent assay (Mitsubishi Kagaku Bio-Clinical Laboratories, Tokyo, Japan). Total RNA was isolated from the infected cellular lysates using an RNeasy minikit (Qiagen, Hilden, Germany) for quantitative reverse transcription-PCR (RT-PCR) analysis of intracellular HCV RNA. The level of intracellular HCV RNA in the RSc cells was $>10^8$ copies/μg total RNA at 4 days postinfection.

Quantitative RT-PCR Analysis. The quantitative RT-PCR analysis for HCV RNA was performed by real-time LightCycler PCR (Roche) as described previously (25). We used the following forward and reverse primer sets for the real-time LightCycler PCR: PML, 5′-GAGGAGTTCCAGTTTCTGCG-3′ (forward), 5′-GCGCCTGGCAGATGGGGCAC-3′ (reverse); β-actin, 5′-TGACGG GGTCACCCACACTG-3′ (forward), 5′-AAGCTGTAGCCGCGCTCGGT-3′ (reverse); HCV-O, 5′-AGAGCCATAGTGGTCTGCGG-3′ (forward), 5′-CTT TCGCGACCCAACACTAC-3′ (reverse); and HCV-JFH1, 5′-5′-AGAGCCAT AGTGGTCTGCGG-3′ (forward), 5′-CTTTCGCAACCCAACGCTAC-3′ (reverse).

Western blot analysis. Cells were lysed in buffer containing 50 mM Tris-HCl (pH 8.0), 150 mM NaCl, 4 mM EDTA, 1% Nonidet P-40, 0.1% sodium dodecyl sulfate, 1 mM dithiothreitol, and 1 mM phenylmethylsulfonyl fluoride. Supernatants from these lysates were subjected to sodium dodecyl sulfate-polyacrylamide gel electrophoresis, followed by immunoblot analysis using anti-PML (A301-168A-1; Bethyl Laboratories, Montgomery, TX), anti-Chk2 (DCS-273; Medical & Biological Laboratories, MBL, Nagoya, Japan), anti-HCV core (CP-9 and CP-11; Institute of Immunology, Tokyo, Japan), anti-HCV NS5A (no. 8926; a generous gift from A Takamizawa, The Research Foundation for Microbial Diseases of Osaka University, Japan), anti-signal transducer and activator of transcription 3 (anti-STAT3) (BD Bioscience, San Jose, CA), anti-phospho-STAT3 (Tyr705) (Cell Signaling Technology, Danvers, MA) anti-poly(ADP-ribose) polymerase 1 (anti-PARP-1) (C-2-10; Calbiochem), or anti-β-actin antibody (Sigma).

MTT assay. HuH-7 or O cells (5×10^3 cells/well) were plated onto 96-well plates and cultured for 24 h. The cells were treated with ATO, APO, or NaOH for 24, 48, or 72 h and then subjected to the colorimetric 3-(4,5-dimethylthiazol-2-yl)-2,5-diphenyltetrazolium bromide (MTT) assay according to the manufacturer's instructions (cell proliferation kit I; Roche). The absorbance was read using a microplate reader (model 2550; Bio-Rad Laboratories, Hercules, CA) at 550 nm with a reference wavelength of 690 nm.

RL assay. OR6 cells (1.5×10^4 cells/well) were plated onto 24-well plates and cultured for 24 h. The cells were treated with each reagent for 72 h and then subjected to the *Renilla* luciferase (RL) assay according to the manufacturer's instructions (Promega, Madison, WI). A Lumat LB9507 luminometer (Berthold, Bad Wildbad, Germany) was used to detect RL activity.

FL assay. Plasmids were transfected into O cells (2×10^4 cells/well in 24-well plates) using FuGene6 and cultured for 24 h. The cells were treated with or without 1 μM ATO for 24 h, and then firefly luciferase (FL) assays were performed according to the manufacturer's instructions (Promega).

Immunofluorescence and confocal microscopic analysis. Cells were fixed in 3.6% formaldehyde in phosphate-buffered saline (PBS), permeabilized in 0.1% NP-40 in PBS at room temperature, and incubated with anti-PML antibody (PM001; MBL) at a 1:300 dilution in PBS containing 3% bovine serum albumin at 37°C for 30 min. They were then stained with fluorescein isothiocyanate-conjugated anti-rabbit antibody (Jackson ImmunoResearch, West Grove, PA) at a 1:300 dilution in PBS containing bovine serum albumin at 37°C for 30 min, followed by staining with 4′,6-diamidino-2-phenylindole (DAPI) at room temperature for 15 min. Following extensive washing in PBS, the cells were mounted on slides using a mounting medium of 90% glycerin–10% PBS with 0.01% *p*-phenylenediamine added to reduce fading. Samples were viewed under a confocal laser-scanning microscope (LSM510; Zeiss, Jena, Germany).

Measurement of intracellular O_2^- and H_2O_2 production. The intracellular superoxide anion radical (O_2^-) levels were measured with an oxidation-sensitive fluorescent probe, dihydroethidium (DHE) (Invitrogen Molecular Probes), that is highly selective for detection of O_2^- among reactive oxygen species (ROS). DHE is cell permeative and reacts with O_2^- to form ethidium, which in turn intercalates in DNA, thereby exhibiting a red fluorescence. The intracellular hydrogen peroxide (H_2O_2) levels were measured with another oxidation-sensitive fluorescent probe dye, 6-carboxy-2′,7′-dichlorodihydrofluorescein diacetate (carboxy-H_2DCFDA) (Invitrogen Molecular Probes). Carboxy-H_2DCFDA was intracellularly deacetylated with esterase and further oxidized with peroxidase to the fluorescent 2′,7′-dichlorodihydrofluorescein (DCF). The ATO- or BSO-treated O cells were washed with PBS and incubated with 5 μM DHE and 20 μM carboxy-H_2DCFDA in PBS at 37°C for 30 min. Cells were then washed twice with PBS. The DHE or DCF fluorescence intensity was measured using a FACSCalibur flow cytometer. For each sample, 10,000 events were collected. The O_2^- or H_2O_2 levels are indicated as mean fluorescence intensities, which were determined with the CellQuest software (BD Bioscience).

Detection of intracellular glutathione. Intracellular glutathione levels were analyzed using CellTracker Green (5-chloromethylfluorescein diacetate [CMFDA]; Molecular Probes, Invitrogen). CMFDA is a membrane-permeative dye used to determine intracellular glutathione levels. Cytoplasmic esterase converts the nonfluorescent CMFDA to the fluorescent 5-chloromethylfluorescein (CMF), which can then react with glutathione. The excitation peak is at 492 nm, and the fluorescence emission peak is at 517 nm. O cells treated with 1 μM ATO for 72 h were washed with PBS and incubated with 5 μM CMFDA at 37°C for 30 min. The CMF fluorescence intensity was measured using a FACSCalibur flow cytometer. For each sample, 10,000 events were collected. The glutathione levels are given as the relative mean fluorescence intensities, which were determined with CellQuest software.

RESULTS

ATO inhibits HCV RNA replication. First, we quantitatively examined the effect of ATO on the HCV RNA replication in HuH-7-derived O cells harboring a replicative genome-length HCV-O RNA (25). We found that submicromolar concentrations of ATO markedly inhibited genome-length HCV-O RNA replication in the O cells at 72 h after administration (Fig. 1A). The 50% effective concentration (EC_{50}) of ATO required for inhibition of genome-length HCV-O RNA replication was 0.19 μM (Fig. 1A). Consistent with this finding, the expression levels of the HCV core and NS5A proteins were also significantly decreased in the cell lysates of O cells treated with ATO for 72 h (Fig. 1B). In addition, ATO markedly inhibited the replication of the subgenomic replicon RNA (31), with an EC_{50} of 0.48 μM at 72 h after the treatment (Fig. 1C). We next examined the effect of ATO on HCV reproduction by HCV-JFH1 infection (58). The results revealed that ATO significantly inhibited the intracellular RNA replication of HCV-

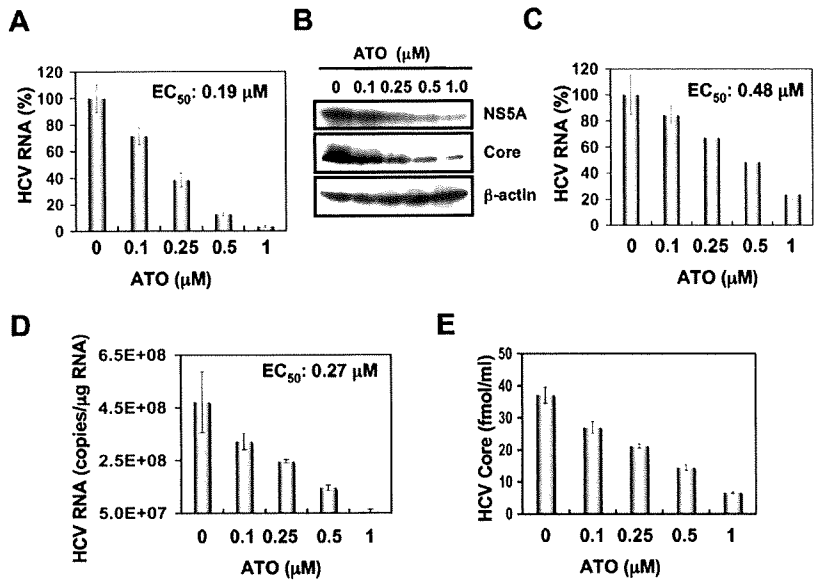

FIG. 1. Inhibition of HCV RNA replication by ATO. (A) The level of genome-length HCV RNA in O cells after the treatment with ATO was monitored by real-time LightCycler PCR. Experiments were done in triplicate and, bars represent the mean percentage of HCV RNA. Error bars indicate standard deviations. (B) HCV core and NS5A protein expression levels in O cells after treatment with ATO. The results of Western blot analysis of cellular lysates with anti-HCV core, anti-HCV NS5A, or anti-β-actin antibody in O cells at 72 h after treatment with ATO at the indicated concentration are shown. (C) The level of subgenomic replicon RNA was monitored by real-time LightCycler PCR. Results from three independent experiments conducted as described for panel A are shown. (D) The level of intracellular genome-length HCV-JFH1 RNA was monitored by real-time LightCycler PCR. RSc cells were pretreated with the indicated concentration of ATO for 13 h, followed by inoculation of the HCV-JFH1 virus, and then the infected cells were further incubated with ATO for 97 h. Results from three independent experiments conducted as described for panel A are shown. (E) The levels of the core protein in the culture supernatants treated as described for panel D were determined by enzyme-linked immunosorbent assay. Experiments were done in triplicate, and bars represent the mean core protein levels.

JFH1, with an EC_{50} of 0.27 μM, as well as the release of core protein into the culture supernatants in HuH-7-derived RSc cells at 97 h after inoculation of the HCV-JFH1 virus (Fig. 1D and E). Thus, we have demonstrated for the first time that ATO can inhibit the reproduction of HCV and particularly HCV RNA replication.

Effect of APO on HCV replication. Arsenic is known to exist in two oxidation states, As(III) in ATO and As(V) in APO. As ATO in the lower valence state has been reported to be more toxic than APO (48), we compared their anti-HCV activities using an OR6 assay system, which was recently developed as a luciferase reporter assay system for monitoring genome-length HCV RNA replication in HuH-7-derived OR6 cells (Fig. 2A) (25). The results showed that APO could not strongly suppress HCV replication at submicromolar concentrations, while ATO strongly inhibited it, with an EC_{50} of 0.33 μM (Fig. 2B and C), indicating that ATO has unique anti-HCV activity. In this context, it is relevant that the expression level of HCV core protein was also remarkably decreased in the cell lysates of O cells treated with ATO, but not those treated with APO, for 72 h (Fig. 2D). Thus, APO seems to be a useful negative probe to clarify the mechanism of the anti-HCV activity of ATO.

ATO does not affect cell growth at submicromolar concentrations. ATO has been reported to induce apoptosis (11, 14, 20, 21, 26–28, 33, 48, 66). Therefore, such an ATO-induced apoptosis may be involved in the anti-HCV activity. To test this possibility, we examined the effect of ATO or APO at various concentrations on cell proliferation by colorimetric MTT assay. In this context, we demonstrated that ATO did not affect the cell proliferation of O cells or the parental HCV-negative HuH-7 cells at submicromolar concentrations (Fig. 3A and E). In contrast, 4 or 8 μM ATO significantly inhibited cell proliferation (Fig. 3B and F). Similarly, APO did not affect the cell proliferation at less than 2 μM (Fig. 3C and D). Consistent with the above results, ATO-treated O cells exhibited normal growth rates and cell viabilities, at least at 1 μM for 72 h (Fig. 3G). Furthermore, we did not observe the cleavage of PARP-1, which is known to be an important substrate for activated caspase 3, in O cells treated with 1 μM ATO at least until 72 h (Fig. 3H), indicating that 1 μM ATO did not induce apoptosis in O cells. Thus, we concluded that the anti-HCV activity was independent of ATO-induced apoptosis or cell toxicity, at least at submicromolar concentrations.

PML and Chk2 are dispensable for the anti-HCV activity of ATO. Since PML is known to be a target of ATO (70), we first examined the subcellular localization of PML in O cells treated with either 1 μM ATO or 1 μM APO for 72 h by means of an anti-PML antibody (PM001; MBL) that can recognize most of the PML splicing variants and is useful for immunofluorescence analysis. The results showed that PML was localized predominantly in punctate nuclear speckles termed PML-NBs in control O cells (Fig. 4A). Interestingly, we noticed that some nuclear PML, but not all, disappeared and was translocated into discrete cytoplasmic bodies in the O cells treated with 1 μM ATO (Fig. 4A). We also observed cytoplasmic translocation of PML in the O cells treated with 1 μM APO for 72 h (Fig. 4A). Furthermore, we observed a similar cytoplasmic translocation of PML in the HCV-negative 293FT or HeLa

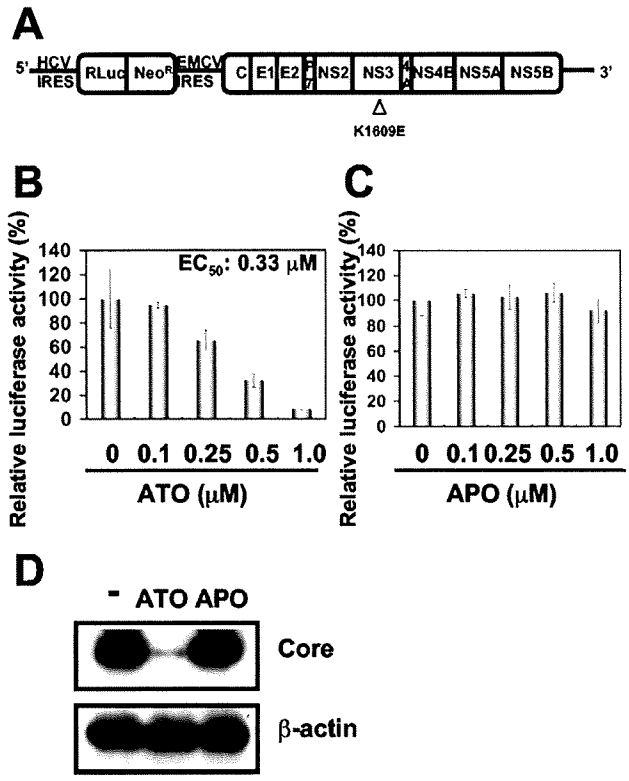

FIG. 2. Effect of APO on HCV replication. (A) Schematic representation of genome-length HCV RNA encoding the RL gene as a reporter (ORN/C-5B/KE RNA) replicated in OR6 cells. The RL is expressed as a fusion protein with neomycin phosphotransferase (Neo^R). The position of an adaptive mutation, K1609E in NS3, is indicated by an open triangle. (B) Effect of ATO on genome-length HCV RNA replication. At 72 h after treatment of OR6 cells with ATO at the indicated concentrations, the replication level of HCV RNA was monitored by the RL assay. The relative RL activity is shown. The results shown are means from three independent experiments. Error bars indicate standard deviations. (C) Effect of APO on genome-length HCV RNA replication. At 72 h after treatment of OR6 cells with APO at the indicated concentrations, the replication level of HCV RNA was monitored by the RL assay as described for panel B. (D) HCV core protein expression level in O cells after treatment with either ATO or APO. The results of Western blot analysis of cellular lysates with anti-HCV core or anti-β-actin antibody in O cells at 72 h after treatment with either 1 μM ATO or 1 μM APO are shown.

cells after the treatment with ATO (data not shown). Thus, we concluded that the cytoplasmic translocation of PML after the treatment with ATO was not associated with anti-HCV activity. Next, Western blot analysis to compare PML expression in the lysates of O cells treated with 1 μM ATO or 1 μM APO for 72 h was performed using another anti-PML antibody, A301-168A-1 (a gift from Bethyl Laboratories), which can recognize the longest isoform, PML I, but not shorter PML isoforms such as PML VI and which has been proven useful for Western blot analysis. Consistent with the previous finding that ATO promotes PML degradation (70), the expression level of the PML I protein was lower in the ATO-treated O cells than in the APO-treated O cells (Fig. 4B), suggesting that PML degradation by ATO is associated with anti-HCV activity. To further examine whether PML is directly involved in the anti-HCV activity of ATO, we used lentiviral vector-mediated RNA interference to stably knock down PML in the O cells. To express an shRNA targeted to all PML isoforms (56), we used the VSV G-pseudotyped HIV-1-based vector system (1, 42, 71). We used the puromycin-resistant pooled cells at 10 days after the lentiviral transduction in this experiment. Immunofluorescence and Western blot analysis demonstrated a very effective knockdown of PML in the O cells (Fig. 4C and D). We quantitatively examined the level of HCV RNA in the PML knockdown O cells treated with or without either 1 μM ATO (Fig. 4E) or 1 μM APO (Fig. 4F) for 72 h. The results showed that the replication level of genome-length HCV-O RNA in the untreated PML knockdown cells was similar to that in control cells (Fig. 4E), suggesting that PML is dispensable in HCV RNA replication. Importantly, ATO effectively inhibited the HCV RNA replication in both the PML knockdown cells and control cells compared with that of the APO-treated cells (Fig. 4E and F). Thus, we concluded that PML was dispensable for the anti-HCV activity of ATO. Since the Chk2 checkpoint kinase has recently been implicated in ATO-induced apoptosis and in association with PML (27, 63, 64, 66), we examined the anti-HCV activity in the ATO-treated Chk2 knockdown O cells (3). As we previously described, Western blot analysis demonstrated very effective knockdown of Chk2 in O cells (Fig. 4G). Accordingly, we examined the level of HCV RNA in Chk2 knockdown cells treated with or without either 1 μM ATO (Fig. 4H) or 1 μM APO (Fig. 4I) for 72 h. Consistent with our recent finding that Chk2 is required for HCV RNA replication, the replication of genome-length HCV RNA in the untreated Chk2 knockdown cells was remarkably suppressed (Fig. 4H). However, ATO strongly inhibited the HCV RNA replication in the Chk2 knockdown cells compared with that in the APO-treated Chk2 knockdown cells (Fig. 4H and I), suggesting that Chk2 is not implicated in the anti-HCV activity of ATO.

Effect of ATO on the stress-signaling pathways. To date, the focus has been on PML and PML-retinoic acid receptor α as major targets of ATO (70). On the other hand, arsenic has been reported to modulate other cell-signaling pathways, especially stress-responsive transcription factors, such as nuclear factor κB (NF-κB), activator protein 1 (AP-1), and STAT3 (12, 37, 38, 62). Therefore, we examined the involvement of several stress-responsive pathways in the anti-HCV activity of ATO by luciferase-based reporter assays or Western blot analysis using an antibody which specifically recognizes STAT3 phosphorylated at tyrosine 705. Although it has been reported that ATO inhibited the NF-κB signaling pathway through a direct interaction with IKKβ at a high concentration (more than 10 μM) (29), neither 1 μM ATO nor 1 μM APO affected the endogenous NF-κB transcriptional activity in the present study (Fig. 5A and B). Conversely, ATO at least slightly stimulated mitogen-activated protein kinase kinase kinase (MEKK)-mediated NF-κB activation (Fig. 5A and B). Since NF-κB activation has been shown to stimulate HCV replication (60), the NF-κB pathway would seem not to be essential for the anti-HCV activity of ATO. Next, regarding the AP-1 signaling pathway, both ATO and APO are known to activate c-Jun N-terminal kinase (JNK) (45). Importantly, there was no stimulation of JNK activity at a dose below 30 μM (45). In fact, 50 μM ATO but not 50 μM APO strongly stimulates AP-1 activity by in-

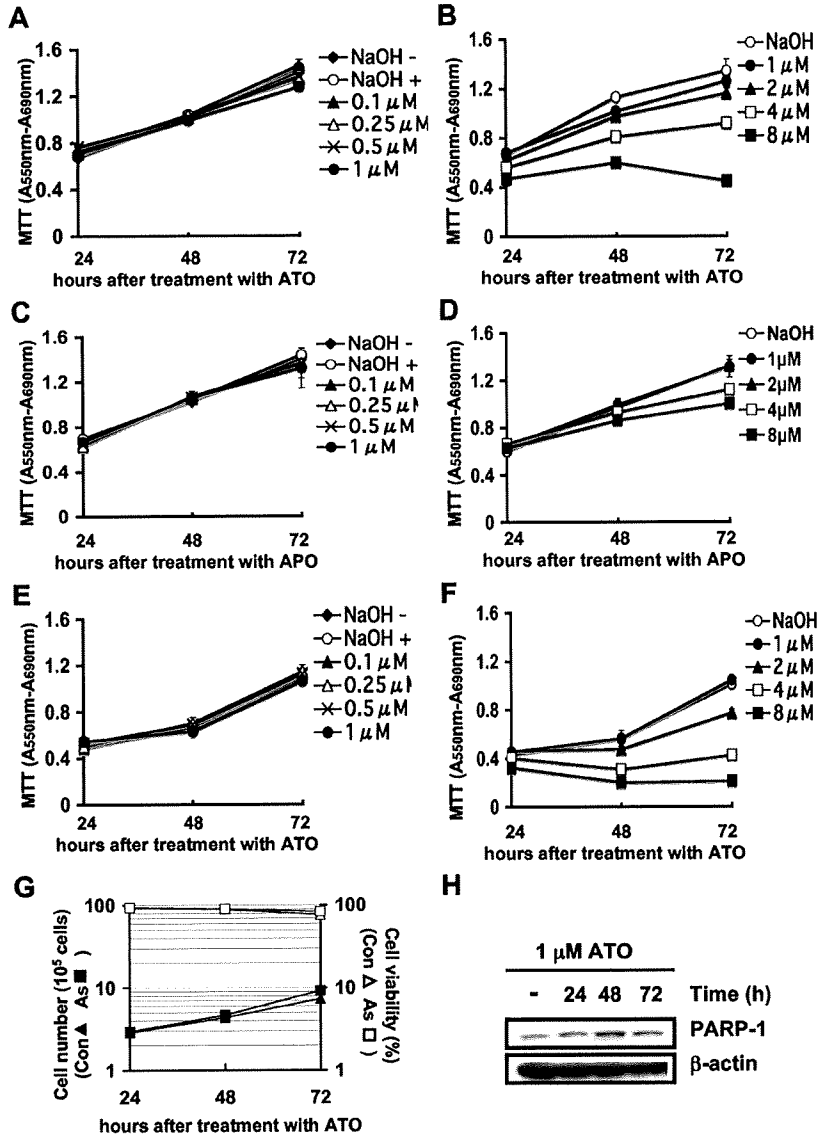

FIG. 3. Effect of ATO on cell growth and viability. (A and B) MTT assay of O cell lysates at the indicated times after treatment with ATO at various concentrations. NaOH (10 μM) was used as the solvent for ATO. The results shown are means from three independent experiments. Error bars indicate standard deviations. (C and D) MTT assay of O cell lysates at the indicated times after treatment with APO at various concentrations. (E and F) MTT assay of HuH-7 cell lysates at the indicated times after treatment with ATO at various concentrations. (G) Growth curve and viability of O cells after treatment with either 10 μM NaOH (Con) or 1 μM ATO (As). (H) Western blot analysis of cellular lysates with anti-PARP-1 or anti-β-actin antibody in O cells at the indicated times after treatment with 1 μM ATO.

hibiting a JNK phosphatase (10). Consistently, we found that both 1 μM ATO and 1 μM APO had a marginal effect on the AP-1 signaling pathway (Fig. 5C and D), suggesting that the AP-1 pathway is also not involved in the anti-HCV activity of ATO. Regarding the STAT3 signaling pathway, ATO has been reported to inhibit the phosphorylation of the STAT3 tyrosine at 705, leading to inactivation of the JAK-STAT signaling pathway (12, 62). In contrast, it has been reported that HCV constitutively phosphorylates and activates STAT3 (49, 59, 67). In this context, we observed constitutive tyrosine phosphorylation of STAT3 in untreated O cells (Fig. 5E). Furthermore, the marginal effect of 1 μM ATO on STAT3 phosphorylation and interleukin-6-mediated STAT3 activation was also observed (Fig. 5E and F). Taken together, these results at least suggest that the NF-κB, AP-1, and STAT3 pathways may not be associated with the anti-HCV activity of ATO at submicromolar concentrations.

The anti-HCV activity of ATO is associated with the glutathione redox system and oxidative stress. Finally, we focused on the involvement of the glutathione redox system and oxidative stress in the anti-HCV activity of ATO. For this, we analyzed the HCV replication level after combination treatment with ATO and antioxidants such as NAC and vitamin C using the OR6 assay system. When OR6 cells were treated with